# MYOFIBRILLAR REGULATORY MECHANISMS OF STRETCH ACTIVATION IN MAMMALIAN STRIATED MUSCLE

---

A Thesis presented to

the Faculty of the Graduate School

at the University of Missouri-Columbia

---

In Partial Fulfillment

of the Requirements for the Degree

Master of Sciences

---

by

JOEL C. ROBINETT

Dr. Kerry McDonald, Thesis Supervisor

May 2017

The undersigned, appointed by the dean of the Graduate School, have examined the thesis entitled:

MYOFIBRILLAR REGULATORY MECHANISMS OF

STRETCH ACTIVATION IN MAMMALIAN STRIATED MUSCLE

presented by Joel Robinett,

a candidate for the degree of Master of Science,

and hereby certify that, in their opinion, it is worthy of acceptance.

Kerry S. McDonald

Alan R. Parrish

Kenneth S. Campbell

Timothy L. Domeier

# Acknowledgements

I would like to thank my thesis advisor, Dr. Kerry McDonald, who has instilled in me a desire to research and understand muscle through an unmatched enthusiasm for his work. I know that I have become a better researcher from simply observing his drive and passion for muscle physiology. He has created an easy-going environment in the lab, while still maintaining an unyielding desire to research. I consider myself lucky to have trained under his advisement. So too, I would like to thank Dr. Laurin Hanft who has been essential to my progression in the laboratory through her willingness to lend a helping hand whenever needed, for which I am very grateful. I also thank the members of my Masters committee, Drs. Kenneth Campbell, Alan Parrish, and Timothy Domeier, for their helpful insights and critiques during my tenure in the Master program. I thank Adam Veteto for his guidance and direction in both the laboratory and the program. He has been very influential during my progression through the graduate program.

# Table of Contents

# List of Tables

# List of Figures

# Abstract

Stretch activation is described as a delayed increase in force after an imposed stretch. This process is essential in the flight muscles of many insects and is also observed, to some degree, in mammalian striated muscles. The mechanistic basis for stretch activation remains uncertain, although it appears to involve cooperative activation of the thin filaments (12, 80). The purpose of this study was to address myofibrillar regulatory mechanisms of stretch activation in mammalian striated muscle. For these studies, permeabilized rat slow-twitch and fast-twitch skeletal muscle fibers were mounted between a force transducer and motor, and a slack-re-stretch maneuver was performed over a range of $Ca^{2+}$ activation levels. Following slack-re-stretch there was a stretch activation process that often resulted in a transient force overshoot ($P_{TO}$), which was quantified relative to steady-state isometric force. $P_{TO}$ was highly dependent upon $Ca^{2+}$ activation level, and the relative magnitude of $P_{TO}$ was greater in slow-twitch fibers than fast-twitch fibers. In both slow-twitch and fast-twitch fibers, force redevelopment involved a fast, $Ca^{2+}$ activation dependent process ($k_1$) and a slower, less activation dependent process ($k_2$). Interestingly, the two processes converged at low levels of $Ca^{2+}$ activation in both fiber types. $P_{TO}$ also contained a relaxation phase, which progressively slowed as $Ca^{2+}$ activation levels increased and was more $Ca^{2+}$ activation dependent in slow-twitch fibers. These results suggest that stretch activation may not be solely regulated by the extent of apparent cooperative activation of force due to a higher relative level of stretch activation in the less cooperative slow-twitch skeletal muscle fiber. Next, we investigated an additional potential molecular mechanism by regulating stretch activation in mammalian striated muscle. Along these lines, our lab has previously

observed that PKA-induced phosphorylation of cMyBP-C and cTnI elicited a significant increase in transient force overshoot following slack-re-stretch maneuver in permeabilized cardiac myocytes (29). Interestingly, in slow-twitch skeletal muscle fibers MyBP-C but not ssTnI is phosphorylated by PKA (28). We, thus, took advantage of this variation in substrates phosphorylated by PKA to investigate the effects of PKA-induced phosphorylation of MyBP-C on stretch activation in slow-twitch skeletal muscle fibers. Following PKA treatment of skinned slow-twitch skeletal muscle fibers, the magnitude of $P_{TO}$ more than doubled, but this only occurred at low levels of $Ca^{2+}$ activation (i.e., ~25% maximal $Ca^{2+}$ activated force). Also, force redevelopment rates were significantly increased over the entire range of $Ca^{2+}$ activation levels following PKA treatment. In a similar manner, force decay rates showed a tendency of being faster following PKA treatment, however, were only statistically significantly faster at 50% $Ca^{2+}$ activation. Overall, these results are consistent with a model whereby stretch transiently increases the number of cross-bridges made available for force generation and PKA phosphorylation of MyBP-C enhances these stretch activation processes.

# Introduction

The fundamental, functional unit of mammalian striated muscle is the sarcomere, which encompasses three main filamentous components; thick filaments, thin filaments, and the titin filament. The thick filament consists predominantly of myosin molecules and also contains MyBP-C molecules arranged in periodic intervals in each half of thick filaments. The thin filament is comprised primarily of three molecules: actin, troponin, and tropomyosin. The third filament mainly consists of the large protein titin, which extends from the Z-line to the M-line of the sarcomere.

## Thick Filament

### Myosin

The major component of the thick filament is myosin. The myosin molecule is comprised of two globular motors attached to a coiled coil α-helical tail (13). The tail is 156 nm long which includes a 43 nm hinged portion (S2 region) that connects to the S1 (head and neck) region of the molecule (65). Each myosin molecule contains two heavy chains and four light chains (55). The heavy chains embody the tail, neck and head regions and play the primary role in myosin's interaction with actin that underlies contraction. The myosin light chains appear to have more of a structural and regulatory role in striated muscle. In fact, one class of light chains are referred to as regulatory light chains (MLC2) (37, 73), whose phosphorylation has been shown to modulate $Ca^{2+}$ sensitivity of force and rate of force development (50) and its level of phosphorylation has been found to be depressed in heart failure (71, 90). The myosin head is known to interact cyclically with both ATP and actin. ATP hydrolysis is thought to provide the

energy that yields the conformational changes in myosin that generate force and filament sliding in the sarcomere (13). The acto-myosin/ATPase cycle during muscle contraction is as follows:

- ATP binds myosin, myosin rapidly dissociates from actin
- ATP hydrolysis becomes ADP + Pi and myosin forms weakly bound cross-bridges with actin
- Release of Pi elicits a strongly bound force generating cross-bridge
- ADP dissociates from myosin
- Cycle repeats

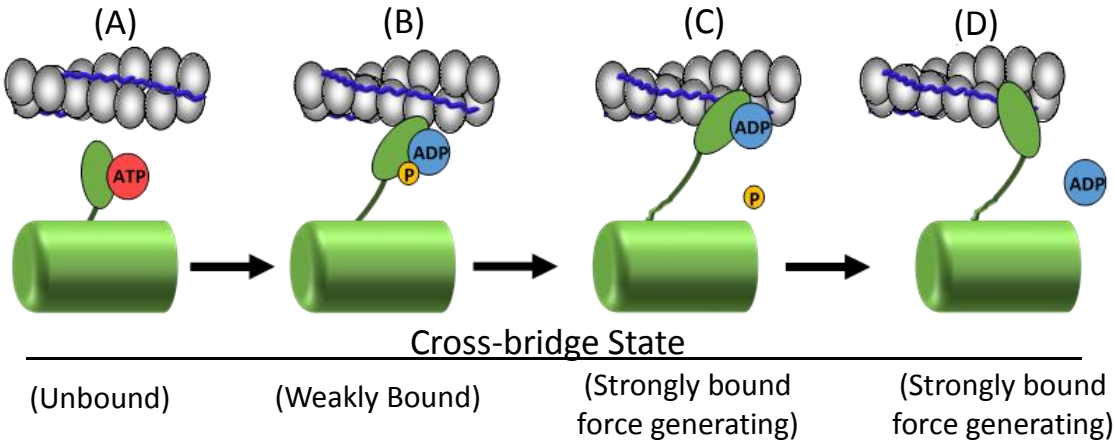


**Figure 1.** *Myosin Cross-bridge Cycle.* The cross-bridge cycle is thought to occur in four states. (A) ATP bound to myosin. Cross-bridge unbound. (B) ATP hydrolysis (ADP + P) leads to formation of weakly bound cross-bridge. (C) Inorganic phosphate is release from myosin head generating a strongly bound non-force generating cross-bridge. (D) Release of ADP causes strongly bound cross-bridges to generate force. Adaption of model from (13).

During isometric contraction, each cross-bridge produces between 2-10 pN of force (13). There is still debate as to if each ATP leads to one cross-bridge cycle (tightly coupled lever arm hypothesis) or if the one ATP can elicit multiple myosin head cycles in a ratchet-like manner (loosely coupled hypothesis) (23).

**Myosin Binding Protein-C**

Myosin binding protein-C was first discovered in 1971 as a protein with a molecular weight that was too small to be a myosin heavy chain, but too big to be a light chain (77). It was thought to be a contaminant of myosin purification preparations and labeled C-protein based on its migration pattern relative to other bands (i.e., third band from the top). C-protein was later found to interact with myosin and re-named myosin binding protein-C (MyBP-C). MyBP-C is a 140-150 kDa elongated, flexible polypeptide that is ~40nm long and ~3 nm wide (31). MyBP-C occurs in sets of 2-3 molecules which are located in the middle third of each half sarcomere in ~7-11 transverse stripes separated by ~43 nm (6). A portion of MyBP-C structure appears lie in parallel to the thick filament while the remainder of the molecule extends radially towards the thin filaments (31). MyBP-C is known to have a strong binding affinity for the S2 and S1 regions on myosin (1, 54, 76) and can bind actin with micromolar affinity (53), which provides a means to alter its interfilament binding and play a modulatory role regulation of myofibrillar contraction. In support of this, ablation of MyBP-C has been shown to speed rates of both force development (38, 79) and sarcomere shortening (34, 38). MyBP-C contains 3 serine residues that are the primary PKA phosphorylation sites (mouse: Ser-273, -282 and -302; human Ser-275, -284, and 304 (2, 5). The exact role of MyBP-C phosphorylation remains uncertain but has been shown to increase the length dependence of contraction (40), speed rates of force development (82), speed relaxation rates (87) and recently increase stretch activation in skinned cardiac myocardial preparations (45).

## Thin Filament

### Actin

Actin is the major component of the thin filament. Actin is comprised of two helical F-actin strands coiled together in an alpha helix with a pitch of ~73 nm (60); the pitch of a helix is defined as the distance of one complete helical rotation. Each F-actin strand is comprised of individual globular actin (g-actin) subunits polymerized together in a series. Each g-actin monomer is roughly 5.46 nm in diameter (75) and consists of four subdomains. Subdomains 1 & 2 project into the periphery for interactions with various proteins while 3 & 4 form the core of the actin filament subdomains (8, 52, 70). Each structural unit of the thin filament, known as the thin filament regulatory unit, consists of 7 actin monomers in a series (55). Actin is anchored to the Z-line of the sarcomere by a barbed capping protein CapZ (63), which is needed for effective force transmission and relative filament sliding (35). Sarcomeric actin's main functional interaction involves its cyclical interaction with myosin heads, which is thought to provide the basis for striated muscle contraction. However, in the intact myofibrillar lattice, actin is not always readily available for interaction with myosin heads. In the relaxed state, myosin binding sites on actin are allosterically inhibited by regulatory molecules on the thin filament (39).

### Troponin Complex

The regulatory molecules include the cable-like tropomyosin molecule and troponin complexes, which together act as Ca2+ sensitive regulators of contraction. The troponin (Tn) complex is comprised of three molecules, troponin C (TnC) which binds $Ca^{2+}$, troponin I (TnI) which is the inhibitory molecule, and troponin T (TnT) which

binds to tropomyosin (Tm). There is one troponin structure per thin filament regulatory unit (23). TnC is a 17 kDa dumbbell shaped molecule that contains EF hands (helix-loop-helix structure) which are $Ca^{2+}$ binding sites (32). Troponin I, an inhibitory molecule (30), ranges in size from 27-31 kDa depending on its isoform (44). The cardiac isoform of TnI contains a 30 amino acid N-terminal extension which contains several phosphorylation sites (27). The third subunit of troponin is TnT which is a ~18.5 nm molecule that has been described as the "glue" of the regulatory complex together (86). The COOH-terminus of TnT is located in the globular region on Tn, while the $NH_2$-terminus is extended along the Tm (86). PKA-induced phosphorylation of cTnI at the serine 23/24 residues elicits faster relaxation rates due in part to an allosteric effect that reduces the $Ca^{2+}$ binding affinity of cTnC, eliciting more rapid $Ca^{2+}$ dissociation from cTnC and removal from the cytosol (67). The serine 23/24 residues are absent in the skeletal isoforms of TnI. TnT is thought to contribute to cooperative activation of force development via its interaction and influence on Tm (22).

**Tropomyosin**

The final major component of the thin filament is Tm. Tropomyosin is a ~ 42 nm long dimer in a coiled coil alpha helix (23). There is one Tm molecule per actin filament regulatory unit (7 G-actin) (23), as well as one Tm filament per F-actin strand, yielding two Tm filaments per thin filament. Tropomyosin molecules arrange in a head-to-tail configuration with a periodicity of 38.5 nm along actin (23). When first discovered, Tm was thought to be a precursor for myosin (3); however, it is now thought that tropomyosin's main function is to regulate contraction via inhibition of the actin myosin interaction (39). In relaxed muscle, tropomyosin lies in the groove of the subdomain 1 of

actin monomers on each of the actin filaments; this is thought to sterically inhibit myosin binding to actin subdomain (23). Phosphorylation of Tm serine 283 causes a straightening and stiffening of the head-to-tail configuration of Tm (41), which is thought to elicit greater thin filament activation via increased level of cooperative activation. Further evidence of the head-to-tail overlap's contribution was seen as a decrease in cooperativity following removal of overlap (56). There are three different states that tropomyosin can exist in, blocked, closed, and open. The transition between these states is driven by $Ca^{2+}$ and the presence of strongly bound cross-bridges (SBXB). The tropomyosin transitions from the blocked state to the closed state following the introduction of $Ca^{2+}$. $Ca^{2+}$ enters the sarcomere, binds to TnC causing conformation changes in troponin which leads to tropomyosin shifting its position into the closed state. Once in the closed state, myosin heads can then strongly bind to actin which transition the tropomyosin to its open state which leads to further contraction.

## Titin Filament

Titin is comprised of extensible and non-extensible regions. The extensible region of titin is comprised of tandem immunoglobulin (Ig) repeats and a PEVK region (rich in proline, glutamate, valine, and lysine) (25). There is evidence that the titin molecule binds to both the thin and thick filaments as it spans the entire length of the half sarcomere (z-line to m-line) (24, 25). Since titin binds to several molecules within the sarcomere, it provides a scaffolding for proper interfilament spacing (89). When first discovered titin was thought to be a collection of polypeptides that formed into a protein complex (92); however, titin is now known to be a protein derived from a single gene that is ~3800 kDa, spans the entire half-sarcomere, and is thought to play a major role in

determining passive force in striated muscle (25). In mammalian heart there are two different isoforms of titin: N2B (a shorter isoform with high passive force) and N2BA (a longer isoform with low passive force) (25). PKA-mediated phosphorylation of titin has been shown to reduce passive force while PKC mediated phosphorylation tends to stiffen titin and increase passive force implicating an important modulatory role of titin in both passive extension and recoil of the sarcomere (18, 25).

## $Ca^{2+}$ Regulation of Contraction

As described above muscle contraction has been canonically thought to be regulated by $Ca^{2+}$ activation of the thin filament (Fig. 2). The process of $Ca^{2+}$ regulation of skeletal muscle contraction is summarized as follows (23, 55):

- Action potential causes release of ACh from the motor nerve
- ACh binding to motor end plates elicits depolarization
- Action potentials propagate along sarcolemma
- Voltage gated sarcolemma channels physically interact to open SR $Ca^{2+}$ channels
- $Ca^{2+}$ released from the sarcoplasmic reticulum
- $Ca^{2+}$ binds Troponin C
- Change in conformation of TnC, TnI, and TnT
- TnT moves Tropomyosin which unveils the myosin binding site on actin monomers
- Myosin binds actin (cross-bridge)

- Cross-bridge power stroke driven by free energy of ATP (see ATP/myosin cross-bridge cycle step by step process)

- $Ca^{2+}$ detachment from TnC
- $Ca^{2+}$ reuptake by the SR
- Detachment of remaining cross-bridges
- Muscle Relaxation

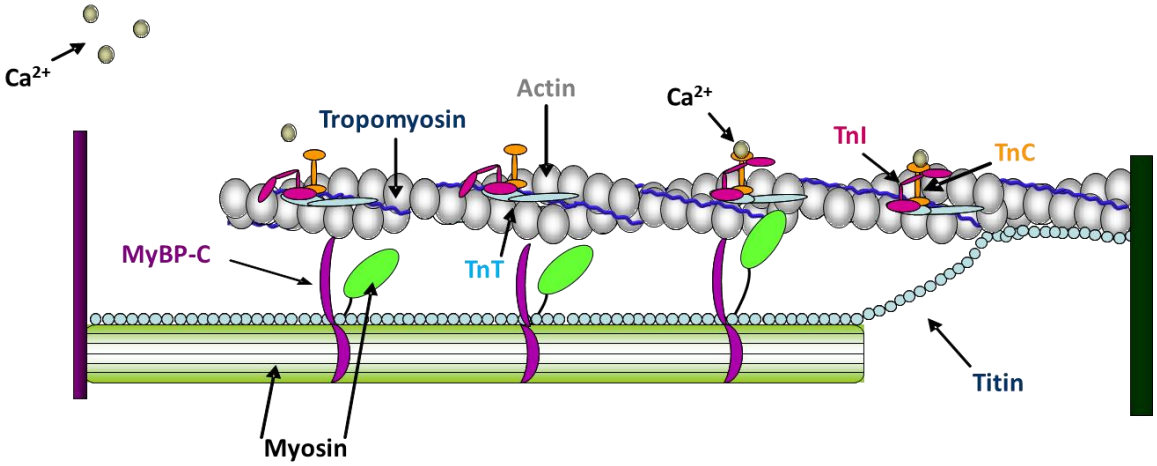


**Figure 2.** *Thin Filament Regulation of Contraction.* Half sarcomere model of $Ca^{2+}$ regulation of contraction. $Ca^{2+}$ (tan) binds to TnC (orange) which cause a change in confirmation of Tnc and TnI (pink). Tm (blue) undergoes an azimuthal shift exposing the active binding sites on actin (gray), which allows myosin heads (green) to bind to actin and generate force.

## Dual-Filament Regulation of Contraction

A novel model of muscle contraction involves dual-filament regulation (42). According to this model the thin filament is still primarily regulated by $Ca^{2+}$, but in addition the thick filaments can be modulated at least in part by strain of stress imparted on them. The thick filament is modeled to exist in three transition states:

- In a super-relaxed state (zero activating $Ca^{2+}$ and no external load), both the thin and thick filaments are in the OFF state (Fig. 3a).

- After the filaments are exposed to $Ca^{2+}$ and the thin filaments are activated, there is population of cross-bridges that are modeled to be constitutively primed for activation. These cross-bridges exclusively are thought to engage the thin filament when the load on the muscle is very low such as when sarcomeres shorten at very high (near maximal) rates (Fig. 3b). In this case, it is thought that less than 5% of the myosin motors are necessary to drive shortening (59), which is the population of cross-bridges that are modeled to be constitutively ON or primed (Fig. 3, green ellipses).
- The third state of the thick filament arises when an external load (either elicited by high stress or strain) is applied to the muscle. In this case the constitutively ON cross-bridges generate stress in the thick filament, which, in turn, releases a population of cross-bridges motors from the OFF state (Fig. 3c). It is only in this state that full isometric force can be produced.

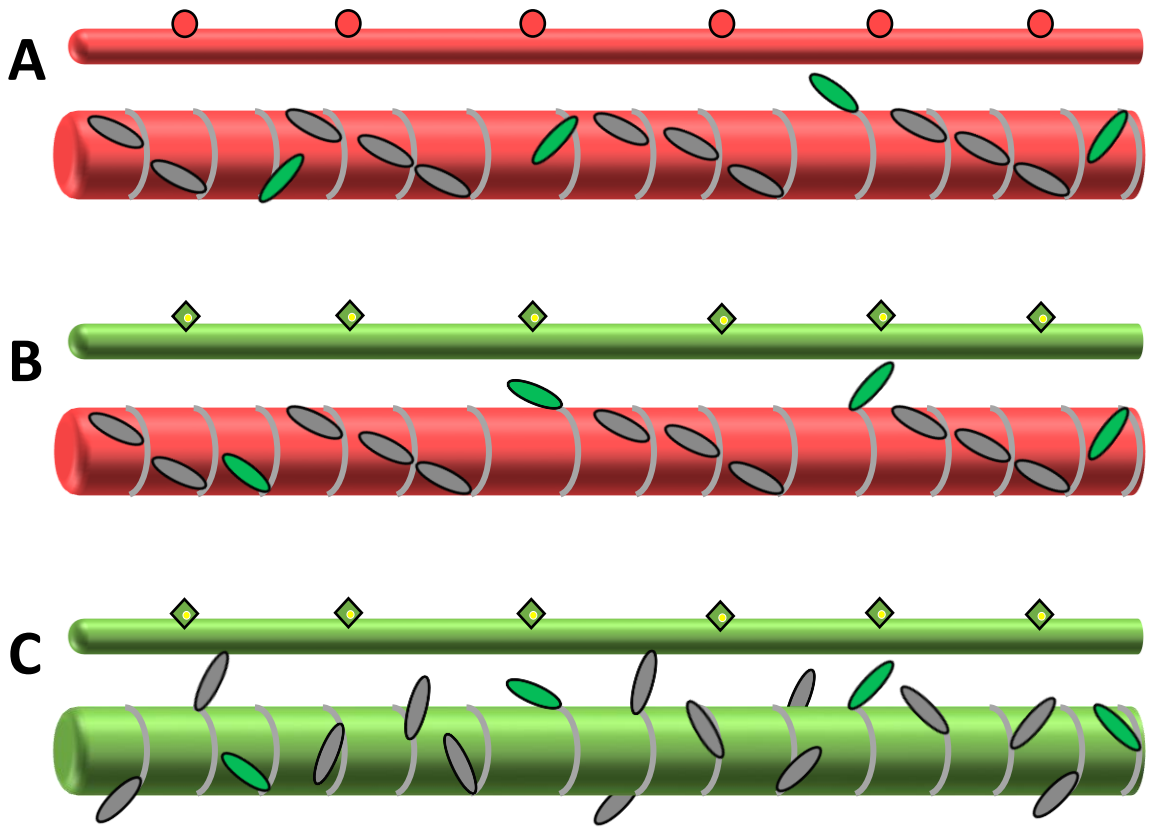


**Figure 3.** *Dual Filament Regulation of Muscle Contraction.* **A.** Resting muscle. Thin and thick filament both in OFF state (red). **B.** Muscle under low load $Ca^{2+}$ activation. Thin filament in ON state (green) while thick filament remains in OFF (red) state, except constitutively ON myosin heads (green ellipses). **C.** Muscle under high load $Ca^{2+}$ activation. Thin and thick filament both in ON state (green). Adaption of model from (42).

## Insect Flight Muscle

Insect flight muscles (IFM) are divided into two major groups, synchronous and asynchronous muscles. Synchronous flight muscles have a 1:1 ratio of neural signals to contractions. Each contraction of synchronous flight muscle is initiated by intracellular $Ca^{2+}$ release and terminated by SR $Ca^{2+}$ reuptake, which is similar to mammalian striated muscle. However, asynchronous flight muscles are divergent. The have roughly a 1:10-40 ratio of neural signal inputs to muscle contractions (46). Asynchronous IFM perform oscillatory wing beats at such a frequency (up to ~500 Hz (46, 93)) that sarcoplasmic

reticulum (SR) $Ca^{2+}$ release and reuptake would not be able to keep up, and the addition of more SR to the muscles would be very metabolically costly (36). Therefore, asynchronous IFM has evolved an additional mode of regulation beyond $Ca^{2+}$ oscillations, quantal summation of force, and temporal summation of forces; this mechanism of regulation is known as stretch activation.

Stretch activation in IFM was first observed in the late 1940s when JWS Pringle observed a delayed increase in force after just a slight muscle lengthening (62). Stretch activation since has been vastly accepted as a regulator of asynchronous IFM contraction (10, 36, 43, 58, 61). In order for stretch activation to be optimally utilized in a functional manner by these insects, there must be two antagonistic muscle groups. These muscles groups will work synergistically with each other to elicit stretch activation, i.e. the contraction of one muscle group stretches and thereby activates the other antagonistic muscle group and vice versa (36, 43, 61). The regulation of contraction via stretch activation is thought to occur as follows (10):

- Action potentials originating from neural inputs propagate along the sarcolemma
- $Ca^{2+}$ enters the muscle and is maintained at a low level
- $Ca^{2+}$ activates the thin filament on the agonist muscle group
- Contraction of the agonist muscle group stretches antagonistic muscle group which provide the trigger for its thin filament activation and subsequent contraction while the agonist muscle group deactivates and relaxes

- The contraction and shortening of the antagonist muscle group then stretches the relaxed agonist muscle group (mechanical feedback loop)
- Elicits 10-40 wing beats per neural impulse

IFMs have evolved their sarcomere in several different ways to accommodate this additional regulation of contraction. In IFM, the periodicity of troponin on the thin filament and myosin cross-bridges is 38.7 nm (58), which favors interaction because the preferred myosin binding site on actin is midway between each troponin complex (88). Insects also have two different isoforms of TnI in their muscles, a larger isoform (53kDa) in IFM, while having a smaller isoform (22kDa) in the insect leg muscles (10). The larger, IFM isoform of TnI is referred to as heavy troponin (TnH) (9). The N-terminus of TnH is similar to TnI; however, the C-terminus of TnH is rich in proline, alanine, and glutamic acid similar to Tm. TnH is at all troponin sites on the thin filament and is now known to be the location of troponin bridges. Troponin bridges extend from troponin on the thin filament to the thick filament (58). These bridges occur when myosin heads bind to troponin in "non-target" areas of the thin filament, which causes and inhibition of contraction. However, following stretch of the muscle, these bridges push (or pull) the Tn-Tm complex on actin from a closed position to open (58). IFM also has two isoforms of TnC (64). One of the isoforms, F2 TnC, produces a $Ca^{2+}$ graded isometric contraction similar to that of mammalian striated muscle. However, the other isoform, F1 TnC, which lacks the $NH_2$-teminal $Ca^{2+}$ binding site, is capable of activating the muscle through stretch via interactions with the Tn complex (64). Both isoforms exist in all myofibrils of the insects, but the ratio of F1:F2 in IFM is 10:1.

Recent findings have led to the theory that troponin-myosin bridges are the regulators of stretch activation in IFM (10, 58). A proposed molecular theory of regulation by stretch activation is as follows:

- In a relaxed, $Ca^{2+}$ free state Tm is covering the binding sites on actin, and TnH is extended across the sarcomere to form a troponin bridge with myosin (Fig. 4a)
- Upon exposure to $Ca^{2+}$ (which binds F1 TnC), thin filament is in a partially open state.
- Once sarcomere is stretched, TnH is pulled/pushed away from actin which subsequently moves tropomyosin. This causes actin to be in the active state which allows myosin to bind to the desired binding site and subsequent force generation.
- Upon shortening the thin and thick filaments make the transition to the relaxed or OFF state.

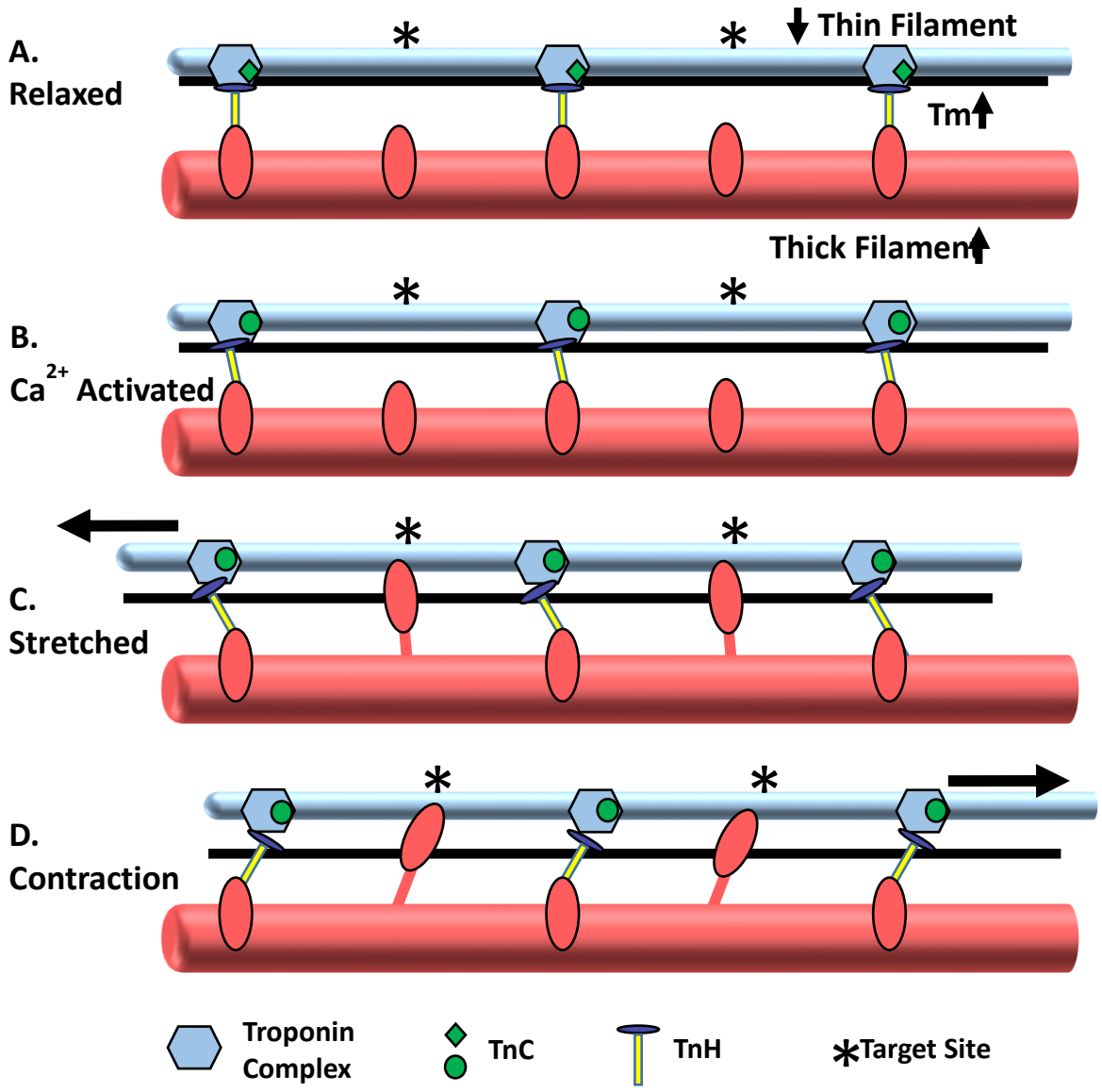


**Figure 4.** *Model of Stretch Activation in IFM.* **A.** Resting muscle, Tm is blocking target sites on actin. Troponin bridges are flanked by target sites. **B.** $Ca^{2+}$ binds to TnC, transitioning the thin filament into the partially open state. **C.** Upon stretch, TnH is pulled away from actin, Tm moves to the open state and crossbridges bind to exposed target sites. **D.** Muscle contracts as the strain is released. The sarcomere will then return to state B. Adaption of model from (58).

Stretch activation in IFM has been found to increase active force greater than 2-fold over isometric force in a length independent manner (93). It is postulated that insect are able to vary the amount of stretch activation being utilized in order to accommodate this broad spectrum of both power per and frequency of wing beat (43, 93).

## Stretch Activation in Mammalian Striated Muscle

While stretch has long been known to regulate contraction in IFM, it is less accepted as a regulator of contraction in striated muscle, even though there has been a considerable number of studies in support of stretch activation in striated muscle dating back to 1970 (68). Rüegg and associates found that a quick 0.2 to 0.5% muscle length stretch of rabbit psoas muscle fibers elicited a transient delayed increases in force. It has since been found that both mammalian cardiac and skeletal muscle has the capacity to utilize stretch activation. In addition, PKA treatment of cardiac and skeletal have been known to modulate force redevelopment and stretch activation (29, 83, 87).

### Cardiac Muscle

Stretch activation has been studied in mammalian cardiac muscle since 1971 (78). Mammalian cardiac muscle utilizes repetitive oscillatory contractions to function in a similar manner as IFM. Due to this, it can be inferred that mammalian cardiac muscle may have similar regulatory mechanisms of contractions (91). However, the underlying mechanism of stretch activation in the heart remains uncertain. There is evidence of stretch activation during systolic contraction, in which early contraction of the ventricular endocardium stretches the epicardium which is later activated. Studies have shown that the ventricle utilizes a torsional contraction in the counter-clockwise direction (viewed

from apex) (16). The endocardium is activated first and contracts in a clockwise direction. The epicardium is activated shortly after and over powers the endocardium in order for the ventricle to contract in a counter-clockwise manner (16). It was postulated that the more forceful epicardial contraction may stretch-activate the endocardium, allowing for a coordinated twisting of the ventricle for optimal wringing and ejection of blood. A potential mechanism of stretch activation during mammalian cardiac cycle:

- Ventricle fill during diastole.
- Upon $Ca^{2+}$ activation, the ventricular endocardium begins to contract in an inner right-handed helix, while the epicardial subsequently activates in an outer left-handed helix.
- The epicardial tends to overpower the endocardium, thought, in part, to be due to elevated regulatory myosin light chain phosphorylation (15), which stretches the endocardium during activation. This is theorized to stretch activate the endocardium to elevate its angular velocity which contributes to optimal wringing and "bottom-up" ejection of blood.

There is considerable evidence for stretch activation in cardiac myofibrillar preparations (16, 29, 78, 80). Unlike the IFM, there is a stretch magnitude dependence of force in mammalian cardiac muscle. For instance, mammalian myocardium exhibited increases in force with increasing sizes of length steps (80) but the amplitude of stretch-activated force in cardiac muscle was much smaller than IFM. Mammalian myocardum has a multiphasic force response to stretch (80). Following a stretch of permeabilized cardiac myocyte preparations there is a multi-phasic mechanical response. First, there is an initial spike in force that coincides with stretch (phase 1), thought to be due to a strain

on the attached cross-bridges, followed by a quick decay of force (phase 2), thought to be the detachment of stained cross-bridges from thin filament, and finally a slow, delayed increase in force (phase 3) which is thought to be a result of stretch activation.

The mechanism of stretch activation in mammalian cardiac muscle remains uncertain although it appears to involve cooperative activation (79). Cooperative activation is a mechanism of force generation by which the binding of one myosin head increases the likelihood of downstream activation of the thin filament. This allows greater activation via an increase in the numbers of strongly bound cross-bridges. Interestingly, stretch activation has been found to increase in mammalian cardiac tissue following PKA treatment (29, 83). PKA phosphorylates cMyBP-C and cTnI (29), which causes an increase in stretch-activated force in mammalian cardiac tissue.

**Skeletal Muscle**

Skeletal muscle tends to operate in a physiologically different manner than cardiac muscle whereby voluntary skeletal muscle contractions can be followed by very long intervals of relaxation (secs to hrs) whereas cardiac muscle functions as pump that requires constant involuntary contraction/relaxation cycles on a second-by-second basis. However, skeletal muscle can function in repetitive oscillatory manner if one considers the contraction/relaxation cycle of a muscle during repetitive activity. When a muscle group and its antagonist muscle group is taken into consideration, a scenario for potential stretch activation arises; for example, during running, contraction of the hamstrings may stretch the quadriceps as they are beginning to be activated for the next cycle of knee extension. If indeed skeletal muscle has the capacity to utilize stretch activation, it is possible that it would occur via the following mechanism in leg muscles:

- Neural signals activate quadriceps muscle group
- Contraction of quadriceps, which stretches hamstrings just when the hamstrings are beginning to be activated
- Stretching yield additional activation of the hamstrings
- Hamstrings contract and shorten, which leads to stretch activation of the quadriceps muscle group

Stretch activation was first evaluated in mammalian skeletal muscle in 1970 on frog semitendinosus and rabbit psoas muscle groups (68). Small stretches of the skeletal muscle elicited a similar delayed increase in force as IFMs. However, the increase in force in skeletal muscle following stretch was substantially smaller than the force increase of IFMs. The delayed increase in force was also transient in skeletal muscle unlike IFM. Stretch activation was theorized to occur in skeletal muscle, which is capable of spontaneous oscillatory contractions (SPOCs) (84), because stretch activation was known to occur during IFM oscillatory contractions. Stretch activation has been found to vary in skeletal muscle based on myosin heavy chain isoforms (20). The various fiber types all have the delayed increase in force following an imposed stretch; however, the kinetics of the force redevelopment were very susceptible to MHC isoforms (20).

One theorized mechanism of stretch activation in skeletal muscle encompasses the SPOCs. SPOCs are theorized to occur via an autonomous interaction between the thick and thin filament that hydrolyzes ATP at low $Ca^{2+}$ levels. SPOCs coupled with decreased lattice spacing upon stretch has been proposed as a possible mechanism of the delayed increase in force (74). Another theorized mechanism of stretch activation in

skeletal muscle involves cooperative activation (12). Slow-twitch skeletal muscle fibers, during steady-state, submaximal $Ca^{2+}$ activations, exhibited a transient force overshoot following a slack-re-stretch maneuver. To study whether recruitment of additional cross-bridges was involved in the transient force overshoot, Campbell (12) implemented small length perturbations on the skinned slow-twitch skeletal muscle fibers during force redevelopment to quantify the stiffness of the fiber, which was used an index in the number of force-generating cross-bridges (17). During force redevelopment, the stiffness of the muscle fiber preparation was highly correlated to the relative force redeveloped implicating that additional cross-bridges perhaps by cooperative recruitment may cause the observed transient overshoot of force (12). If indeed, cooperative recruitment of cross-bridges is the mechanism for transient force overshoot, it stands to reason that fast-twitch skeletal muscle fibers would have greater magnitude of transient force overshoot compared to slow-twitch skeletal muscle fibers since fast-twitch skeletal muscle is known to have a higher relative level of cooperativity compared to the slow-twitch fibers (21, 47).

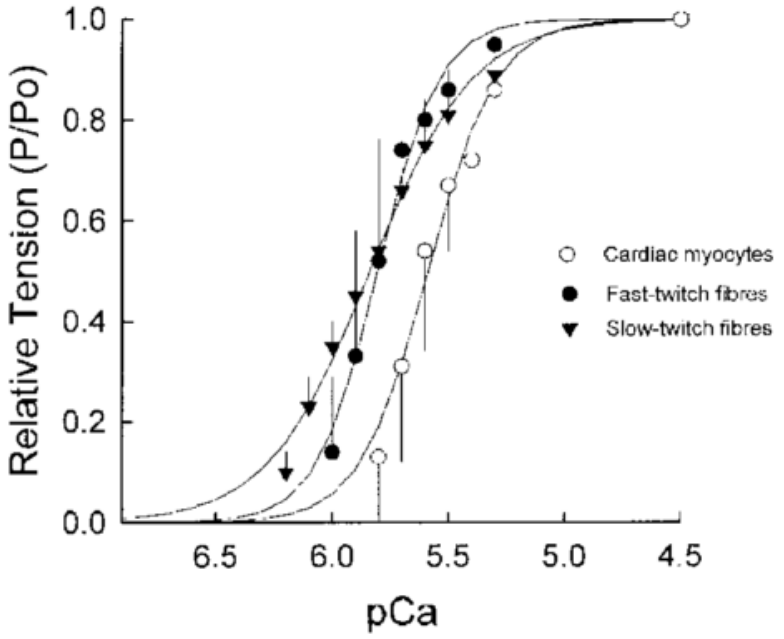


**Figure 5.** *Tension-pCa Relationships in Muscle Types.* Steepness of the tension-pCa curve was assesed at ~50% $Ca^{2+}$-activated forces. Fast-twitch fibers displayed a steeper tension-pCa curve than slow-twitch fibers, indicative of a higher cooperativity of $Ca^{2+}$ activation in fast-twitch fibers. Cardiac myocytes (○), fast-twitch skeletal muscle fibres (●), and slow-twitch skeletal muscle fibres (▼). Taken from (47).

# Hypothesis

If stretch activation is in fact due to cooperative activation of the thin filament, then the magnitude of the transient force overshoot will manifest greater in fast-twitch skeletal muscle fibers compared to slow-twitch fibers due to its higher relative level of cooperative activation, and in order to explore more into the molecular mechanism of stretch activation, we investigated the effects PKA-induced phosphorylation of MyBP-C on the transient force overshoot in slow-twitch skeletal muscle fibers.

# Materials and Methods

## Experimental Animals

All Procedures involving animals were performed in accordance with the Animal Care and Use Committee of the University of Missouri. Male Sprague-Dawley rats (~2-4 months), obtained from Harlan (Madison, WI), were housed in groups of two and provided food and water ad libitum.

## Solutions

Relaxing solutions for permeabilized skeletal muscle fibers contained: 1 mM DTT, 100 mM KCL, 10 mM Imidazole, 2.0 mM EGTA, 4.0 mM ATP, 1 mM (free, 5 total) $MgCl_2$. Minimal $Ca^{2+}$ activating solution (pCa 9.0) for experimental protocol contained: 7.00 mM EGTA, 20 mM Imidazole, 5.42 mM $MgCl_2$, 72.37 mM KCl, 0.01633 mM $CaCl_2$, 14.50 mM PCr, 4.7 mM ATP. Maximal $Ca^{2+}$ activating solution (pCa 4.5) for experimental protocol contained: 7.00 mM EGTA, 20 mM Imidazole, 5.26 mM $MgCl_2$, 60.25 mM KCl, 7.01 mM $CaCl_2$, 14.50 mM PCr, 4.81 mM ATP. A range of $Ca^{2+}$ concentrations for experiments was prepared by varying combinations of maximal and minimal $Ca^{2+}$ solutions. Pre-activating solution contained: 0.5 mM EGTA, 20 mM Imidazole, 5.42 mM $MgCl_2$, 98.18 mM KCl, 0.016 mM $CaCl_2$, 14.50 mM PCr, and 4.8 mM ATP. PKA solution prepared by diluting 1 mg DTT in 100 µL of bottle distilled water. DTT solution was then added to PKA. 100 µL PKA was then diluted in 700 µL minimal $Ca^{2+}$ solution.

## Skeletal Muscle Fiber Preparation

Slow-twitch and fast-twitch skeletal muscle fibers were obtained from Sprague-Dawley rats anaesthetized by inhalation of isoflurane (1mL: 4mL olive oil), and subsequently euthanized by excision of the heart. Slow-twitch skeletal muscle fibers were obtained from the soleus muscle, while the fast-twitch skeletal muscle fibers were obtained from the psoas muscle. The muscles were isolated and placed in relaxing solution. Bundles of muscle fibers were separated and tied to capillary tubes. They were stored in the freezer in 1:1 ratio of relaxing solution and glycerol for up to one month. On day of experiment single fibers were dissected from bundle by gentle pulling fibers from the end of bundle (48).

## Experimental Apparatus

Prior to mechanical measurements the experimental apparatus was mounted on the stage of an inverted microscope (Model IX-70, Olympus Instrument Co., Japan), which was placed upon a pneumatic vibration isolation table. Mechanical measurements were performed using a capacitance gauge force transducer (Model 403-sensitivity of 20 mV/mg and resonant frequency of 600 Hz; Aurora Scientific, Inc., Aurora, ON, Canada). Length changes were presented to one end of the fiber via a DC torque motor (model 308c, Aurora Scientific, Inc.) driven by voltage commands from a personal computer via a 12- or 16-bit D/A converter (AT-MIO-16E-1, National Instruments Corp., Austin, TX, USA) (47). Fibers were attached between the force transducer and length motor by placing the ends of the fibers preparation into stainless steel troughs (25 gauge). The ends of the fiber preparations were secured by overlaying a ~0.5 mm length of 3-0

monofilament suture (Ethicon, Inc.) onto each end of the fiber. The suture secured the fiber into the troughs by two or three loops of 10-0 monofilament (Ethicon, Inc.) as shown in Fig.6. The attachment procedure was performed under a stereomicroscope (+10x zoom). The dimensions of the fiber preparations are summarized in Table 1. Force and length signals were digitized at 1 kHz and stored on a personal computer using Lab-View for Windows (National Instruments Corp.). Simultaneous sarcomere length measurements of force and length were obtained via IonOptix SarcLen system (IonOptix, Milton, MA), which used a fast Fourier transform algorithm of the video image of the fiber.

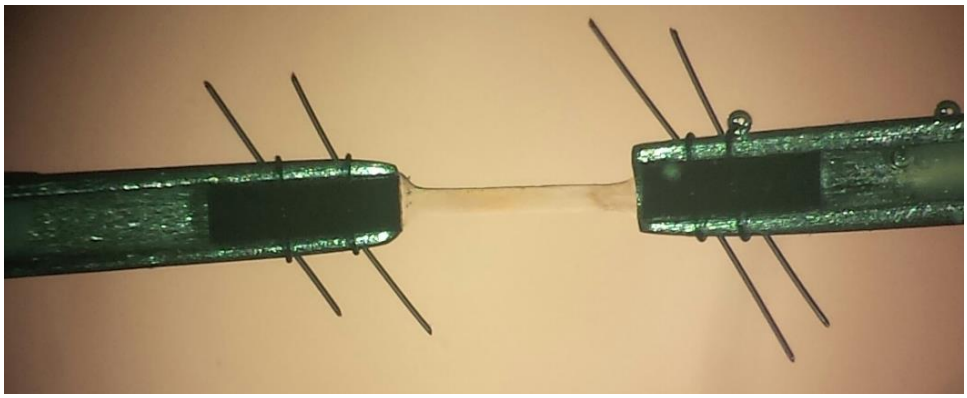

**Figure 6.** *Skinned Fiber Apparatus.* Skinned skeletal muscle fibers were mounted between a length motor and force transducer. Experiment were performed in varying $Ca^{2+}$ activating solutions.

## Slack-Re-stretch Protocol

All mechanical measurements of skeletal muscle fibers were performed at 14 ± 1 °C. Following attachment, the relaxed skeletal muscle fiber preparation was adjusted to a sarcomere length of ~2.40 ± 0.1 nm by manual manipulation of the length micrometer on fiber mount. The preparation was first transferred into pCa 4.5 solution for maximal

activation then subsequently transferred into a series of sub-maximal activating $Ca^{2+}$ solutions, ending back in pCa 4.5 maximal activating solution. At each pCa, steady-state tension was allowed to develop and the cell was rapidly slacked (~15% original muscle length) and re-stretched to original muscle length in order to elicit force redevelopment from zero tension (Fig. 7). The fibers underwent ~3 slack-re-stretch maneuvers at each $Ca^{2+}$ activation level. Forces in sub-maximal activating solutions were expressed as a fraction of force obtained during maximal $Ca^{2+}$ activation. The maximal force value was calculated as an average of maximal force at the beginning and end of the experiment. To assess the effects PKA-induced phosphorylation of MyBP-C on the transient force overshoot, rate of force redevelopment, and transient force decay rate, the aforementioned slack-re-stretch protocol was performed before and after a 60 minute incubation with PKA (Sigma, 0.5 U/ml). $Ca^{2+}$ activating solutions were adjusted in order to elicit desired relative forces (25%, 50%, 75%, and maximal activation); the same sub-maximal activing pCa solutions were used following PKA treatment in the respective fibers. The first part of the protocol for the PKA experiments is the same as the comparative study of skinned slow-twitch muscle fiber preparations. Therefore, the before PKA experimental values are similar to the slow-twitch muscle fiber experimental values.

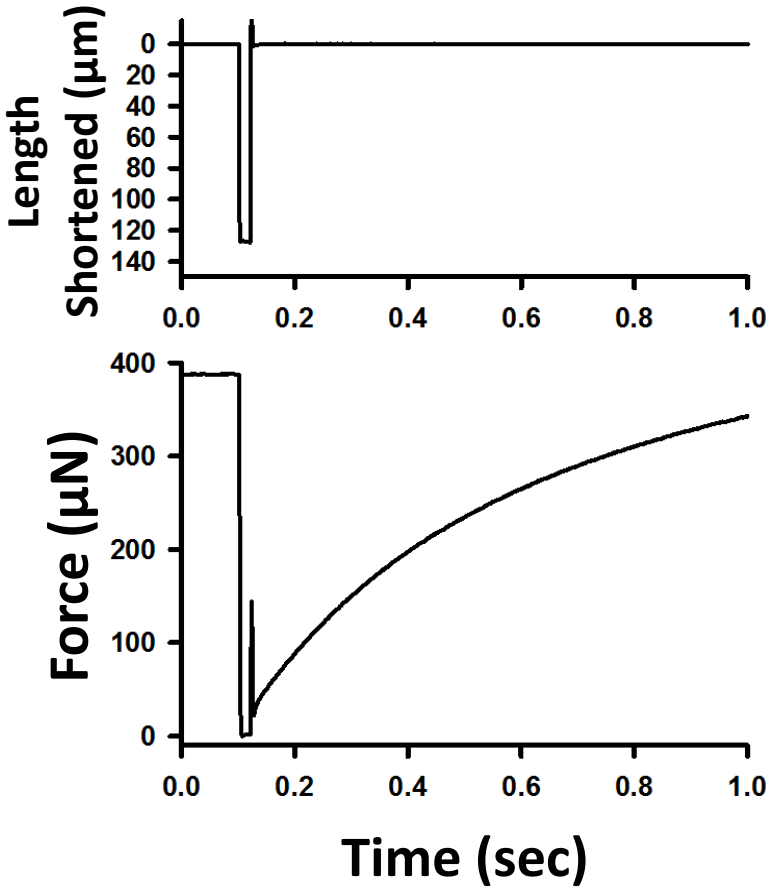


**Figure 7.** *Slack-Re-Stretch Protocol*. Skinned fibers were submerged into $Ca^{2+}$ activating solution. Once isometric force was developed. A ~15% slack was imposed on the muscle fibers, which was held for 20 msec, followed by re-stretch to original muscle length. Force redevelopment was observed over 15-30 sec.

## Data Analysis

Often in the literature, force redevelopment traces are fit with a single exponential equation (12, 29, 81); however, during analysis it was found that often times the force redevelopment traces were better fit with a double exponential equation (Fig. 8). Force was fit with the equation as follows:

$$F = F_r + A(1 - e^{-k_1 x}) + B(1 - e^{-k_2 x})$$

Where F is force during force redevelopment, and $F_r$ is the residual force before redevelopment, and A is the force contributing to the first exponential phase, while $k_1$ is the rate constant of force redevelopment of this first exponential phase, and B is the force contributing to the second exponential phase with a rate constant of $k_2$. Force redevelopment was fit from $F_r$ to maximal transient force elicited.

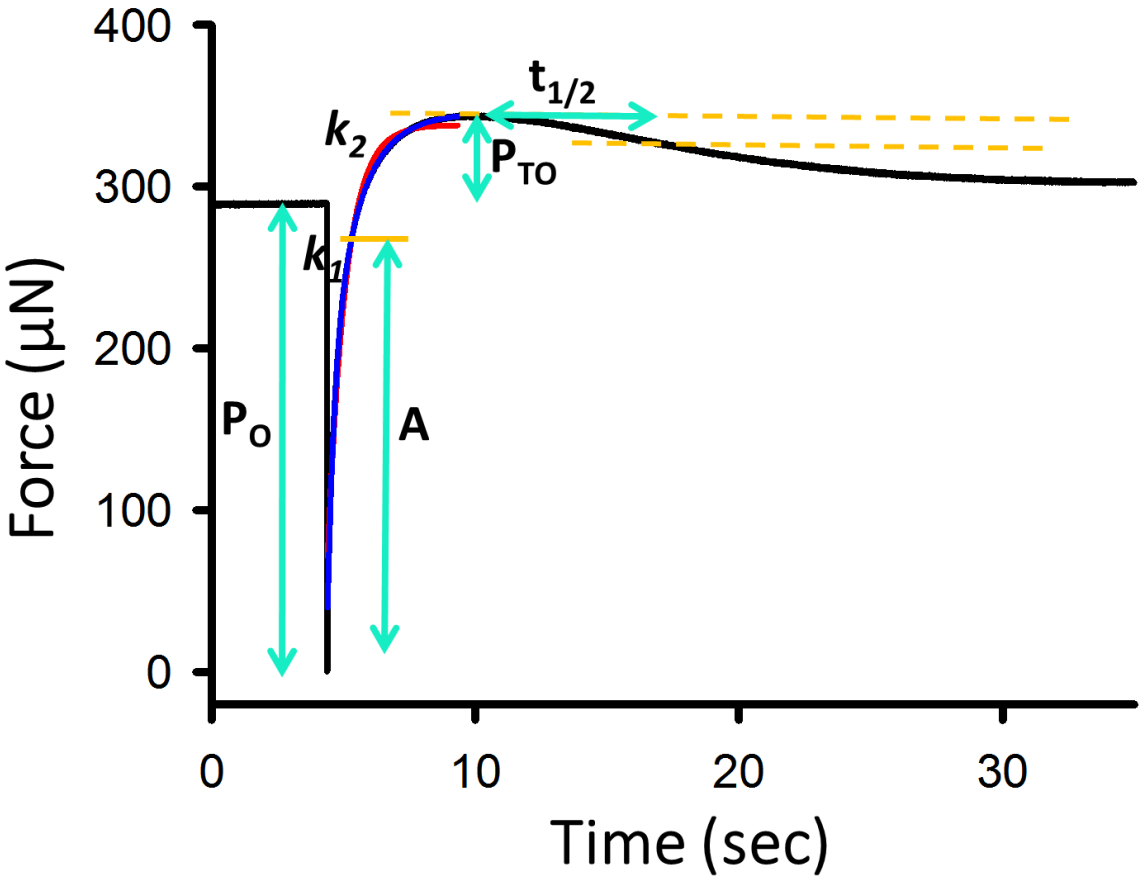


**Figure 8.** *Force redevelopment trace and illustrative definition of annotations.*

Force redevelopment traces elicited various force characteristic values. Once isolated, skeletal muscle fibers were submerged in $Ca^{2+}$ activating solutions and allowed to rise to steady-state isometric force ($P_O$). Following slack-re-stretch maneuver, force

often redeveloped transiently to a maximal force ($P_{TO+O}$). Values for transient force overshoots were calculated by subtracting isometric force from the maximal redeveloped force($P_{TO} = P_{TO+O} - P_O$). Transient force overshoots were analyzed relative to isometric force ($P_{TO}/P_O$).

Rates of transient force decay were calculated as follows:

$$t_{1/2} = time from\ maximal\ force\ to\ when\ Force = \frac{0.95 * (P_{O+TO} - P_O)}{2}$$

## Statistical Analysis

Slow-twitch skeletal muscle fibers were compared to fast-twitch skeletal muscle fibers via Two-way ANOVA. Slow-twitch skeletal muscle fibers before verses after PKA treatment were compared via paired t-test. P-value below 0.05 is considered significant. * denotes significant difference.

# Results

*$Ca^{2+}$ Dependence of Transient Force Overshoot in Skeletal Muscle Fibers*

Stretch activation is described as a delay increase in force following an imposed stretch (61). The underlying mechanism of stretch activation remains unknown although it appears to involve cooperative activation of the thin filament (12, 80). Our first study was to test the theory that stretch activation is regulated by cooperative activation in mammalian striated muscle. This was done by a comparative study of stretch activation in slow-twitch and fast-twitch fibers. As previously stated, stretch activation was hypothesized to be greater in fast-twitch fibers due to their greater relative level of cooperative activation (47). Skinned skeletal muscle fibers (summarized in Table 1)

were activated to elicit 25%, 50%, 75%, and 100% maximal $Ca^{2+}$ activation and once steady-state force was reached, a slack-re-stretch maneuver was performed. Force redevelopment after the slack-re-stretch maneuver was often associated with a transient overshoot of force ($P_{TO}$) (Fig. 9). Both fast-twitch and slow-twitch skinned skeletal muscle fibers exhibited a $Ca^{2+}$ dependence of $P_{TO}$. Submaximal (50%) $Ca^{2+}$ activation elicited the greatest magnitude of $P_{TO}$, while maximal activation elicited the smallest $P_{TO}$.

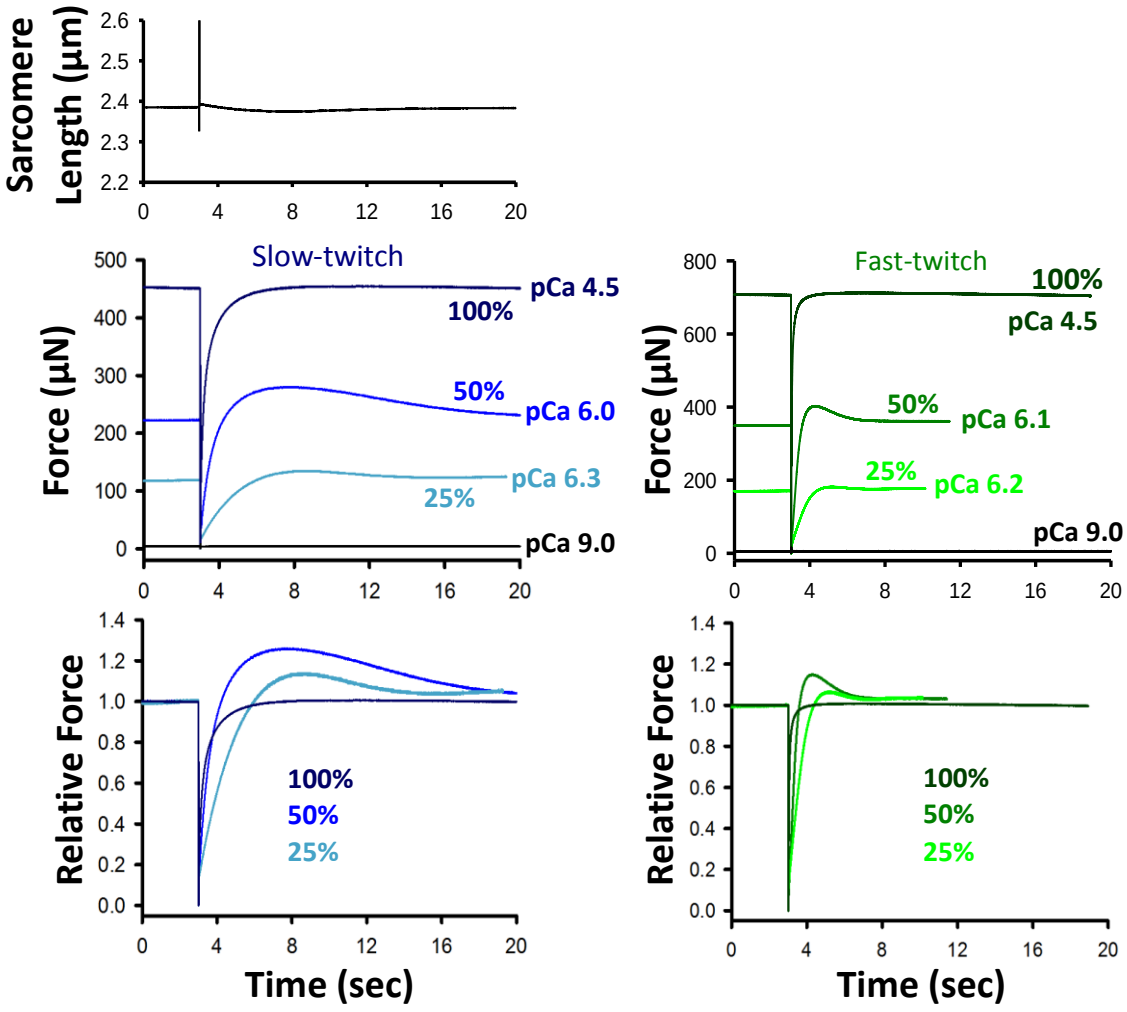


**Figure 9.** *$Ca^{2+}$ dependence of force traces following slack-re-stretch maneuver.* Representative sarcomere length trace. Representative absolute force traces following a slack-re-stretch maneuver from a slow-twitch (blue) and a fast-twitch (green) skeletal muscle fiber. Force traces normalized to the steady-state force before the mechanical perturbation.

Table 1. Skeletal Muscle Fiber Preparation Characteristics

| | Date | Length (μm) | Width (μm) | Force (μN) at pCa 9.0 | Force (μN) at pCa4.5 | Tension ($kN/m^2$) |
|---|---|---|---|---|---|---|
| Slow-twitch Fibers | 1/20/2016 | 1304 | 80 | 1.96 | 683 | 151 |
| | 3/3/2016 | 1000 | 87 | 0.98 | 668 | 125 |
| | 4/6/2016 | 904 | 61 | 1.47 | 339 | 129 |
| | 5/4/2016 | 1009 | 61 | 0.98 | 439 | 167 |
| | 6/14/2016 | 952 | 76 | 2.94 | 594 | 147 |
| Fast-twitch Fibers | 5/31/2016 | 1209 | 87 | 0.98 | 693 | 130 |
| | 6/2/2016 | 709 | 83 | 0.98 | 603 | 125 |
| | 6/7/2016 | 870 | 104 | 1.96 | 1204 | 157 |
| | 6/28/2016 | 1052 | 91 | 0.98 | 916 | 156 |
| Slow-twitch Fibers Before PKA | 7/6/2016 | 970 | 91 | 5.39 | 730 | 125 |
| | 8/26/2016 | 1009 | 61 | 1.47 | 345 | 131 |
| | 11/22/2016 | 1004 | 83 | 4.9 | 625 | 130 |
| | 11/29/2016 | 1304 | 61 | 2.94 | 510 | 196 |
| Slow-twitch Fibers After PKA | 7/6/2016 | 970 | 91 | 2.94 | 703 | 120 |
| | 8/26/2016 | 1009 | 61 | 0.98 | 342 | 130 |
| | 11/22/2016 | 1004 | 83 | 2.45 | 604 | 125 |
| | 11/29/2016 | 1304 | 61 | 1.47 | 500 | 192 |

Sarcomere length was set at 2.40 ± 0.10 μm during $Ca^{2+}$ activations. Solution temperature was set at 14.0 ± 1.0ºC.

In order to compare the capacity for stretch activation between slow-twitch and fast-twitch skeletal muscle fiber types, transient overshoots of force ($P_{TO}$) (i.e. the magnitude of force that transiently redeveloped above steady-state isometric force) were characterized from both fiber types. Contrary to our hypothesis, force redevelopment in slow-twitch fibers elicited greater relative transient force overshoots than the more cooperative fast-twitch fibers over the spectrum of $Ca^{2+}$ activation (see Table 2 for summary). This indicates that slow-twitch skeletal muscle may have a greater capacity for stretch activation than fast-twitch skeletal muscle. However, there was not a fiber-type dependence of $P_{TO}$ at max $Ca^{2+}$ activation which is thought to arise from a lack of additional cross-bridges available for force generation following slack-re-stretch

maneuver. Overall, these results suggest that stretch activation may not be solely regulated by the extent of apparent cooperative activation of force due to a higher relative level of stretch activation in the less cooperative slow-twitch skeletal muscle fiber.

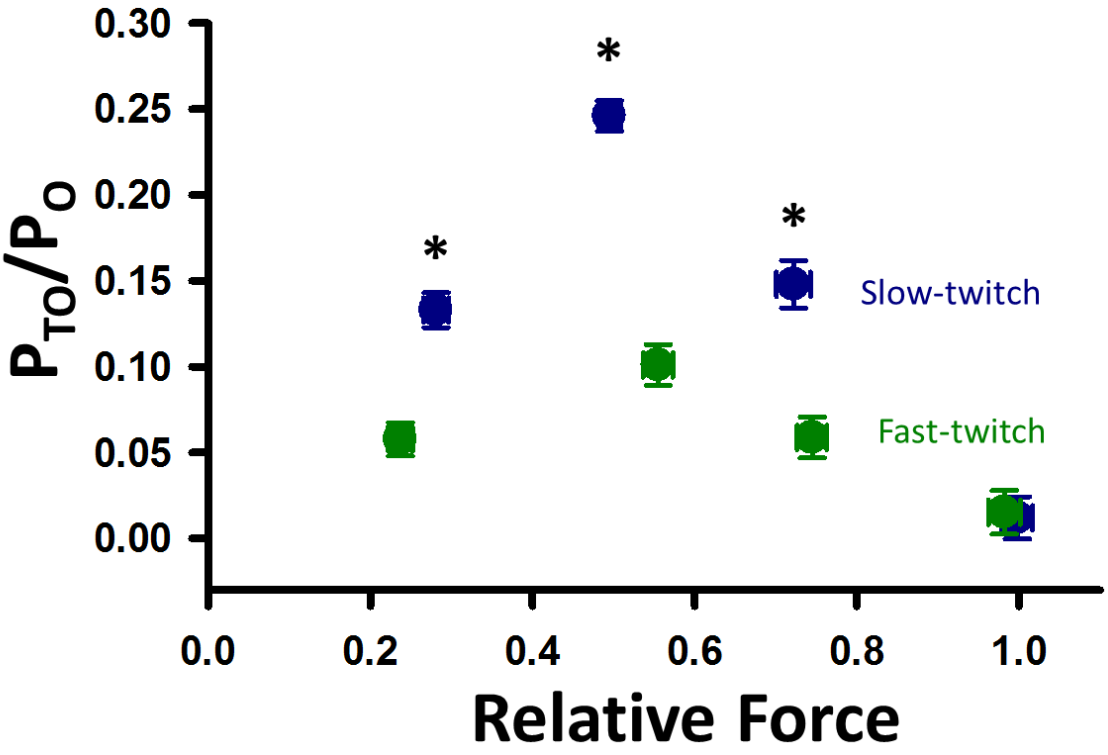


**Figure 10.** *Transient force overshoot ($P_{TO}$) in slow-twitch (blue) and fast-twitch (green) skeletal muscle fibers as a function of $Ca^{2+}$ activation levels.* $P_{TO}$ was expressed as a fraction of steady-state force ($P_O$) before the slack-re-stretch maneuver. Data points are mean ±SEM. By two-way ANOVA, within slow-twitch and fast-twitch fiber groups, all $P_{TO}$ points were significantly different from each other except at ~25% versus ~75% forces. * Slow twitch-fibers had greater relative transient force overshoot than fast-twitch fibers at all relative force values except for 100% force.

*Force Redevelopment Rates*

Force development rates were characterized throughout the entire transient force overshoot process. Force redevelopment traces have mostly been fit with a single exponential equation over a one second time frame (12, 29, 81). We found that force redevelopment over several seconds that includes the transient force overshoot was well

fit with a double exponential equation, which implies two distinct molecular processes are involved in this prolonged force development phase of skeletal muscle myofilament. As seen in Fig. 11, force redevelopment over this time frame often involved a fast phase with the rate constant $k_1$ followed by a slower phase with the rate constant $k_2$. Fast-twitch muscle fibers elicited faster rates of force redevelopment than slow-twitch muscle fibers over the entire range of $Ca^{2+}$ activation. Interestingly, in both fiber types, the two different processes of force redevelopment converge into one process at low $Ca^{2+}$ (Fig. 11) (all values summarized in Table 2). The rate constant of the fast process ($k_1$) was $Ca^{2+}$ activation dependent, while the slower process ($k_2$) was less $Ca^{2+}$ activation dependent. This convergence of force redevelopment processes suggests that at low $Ca^{2+}$ only one of the two molecular processes dominant in its contribution to force generation.

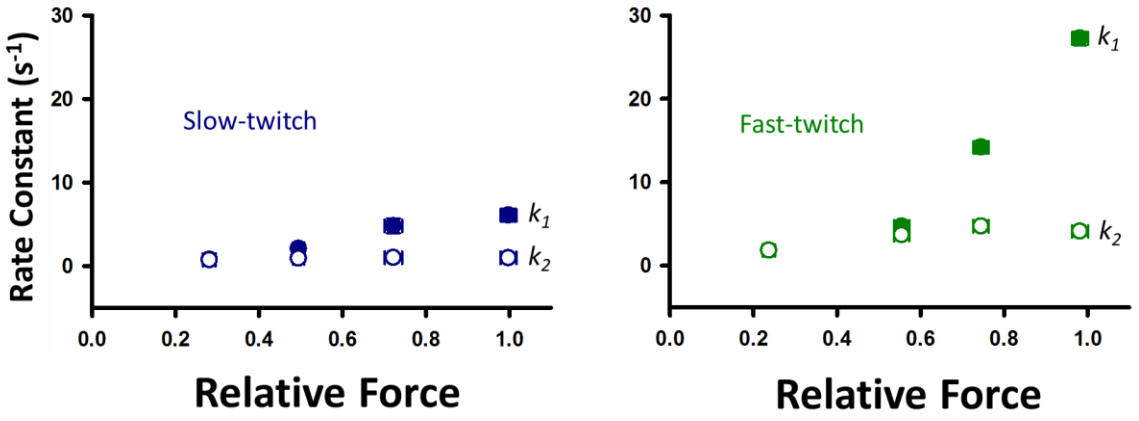


**Figure 11.** *Force redevelopment rates.* Rate constants ($s^{-1}$) from a double exponential ($k_1$ and $k_2$) fit across relative forces in slow-twitch (blue) and fast-twitch (green) fibers. Values for $k_1$ were highly dependent on $Ca^{2+}$ activation levels, while $k_2$ values were similar over the entire range of $Ca^{2+}$ activation levels. Values for $k_1$ at ~75% and ~100% relative force were significantly different from all other values in both fiber types.

*Force Decay Rates*

The rate of force decay was assessed in both slow-twitch and fast-twitch fibers. In this study, force decay rates quantified as the time to half decay of force ($t_{1/2}$). Similar to force redevelopment rates, fast-twitch skeletal muscle fibers had a faster decay rate of the transient force overshoot as shown by a smaller $t_{1/2}$ (all values summarized in Table 2). Slow-twitch muscle fibers had a highly $Ca^{2+}$ activation dependent force decay rate ($t_{1/2}$ was different at all $Ca^{2+}$ activation levels). However, the force decay rate in fast-twitch fibers was much less $Ca^{2+}$ activation dependent ($t_{1/2}$ at max $Ca^{2+}$ greater than other values).

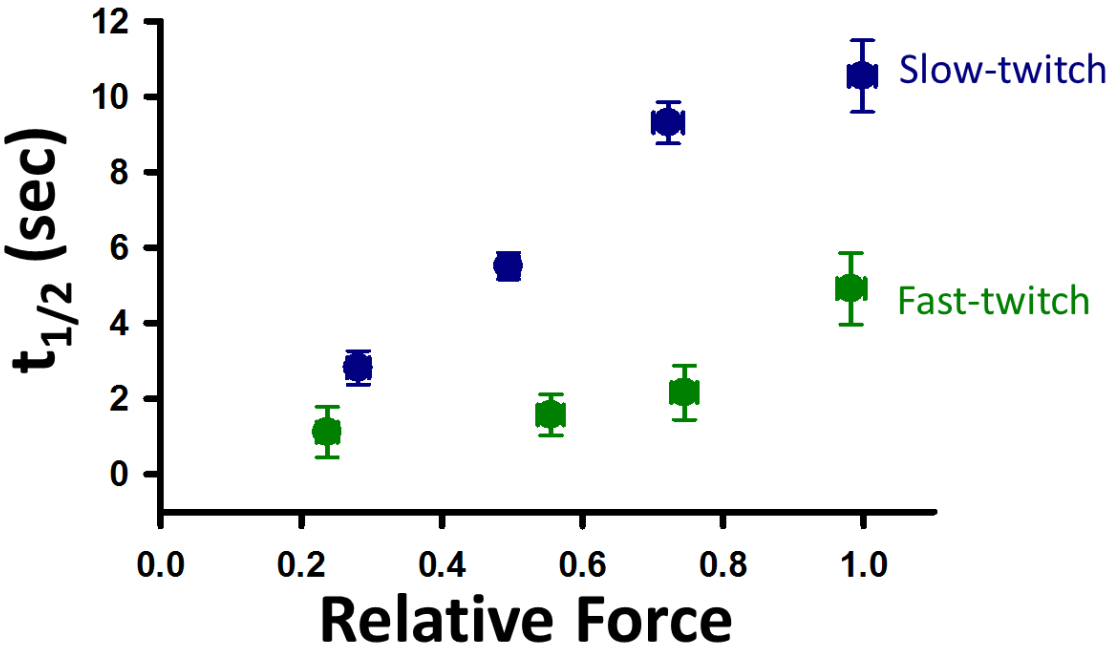


**Figure 12.** *Force decay half-times ($t_{1/2}$) of transient force overshoots.* $t_{1/2}$ was $Ca^{2+}$ activation dependent in a manner qualitatively similar to the $k_1$ rate constant (in Figure 11). In slow-twitch twitch fibers, the $t_{1/2}$ at ~50% relative force was significantly different from all other values. In fast-twitch fibers, the $t_{1/2}$ at ~100% relative force was significantly greater than all other values.

Table 2. Characteristics of Force Redevelopment in Slow-twitch vs. Fast-twitch Muscle Fibers

| | **Rel. Force (%)** | $P_O/P_{4.5}$ (%) | $P_{TO}/P_O$ (%) | $k_1$ ($s^{-1}$) | $k_2$ ($s^{-1}$) | $t_{1/2}$ (sec) |
|---|---|---|---|---|---|---|
| Slow-twitch Fibers | **25** | 28.1 | 13.3 | 0.77 | 0.72 | 2.82 |
| | **50** | 49.5 | 24.6 | 2.07 | 0.91 | 5.51 |
| | **75** | 72.2 | 14.8 | 4.79 | 0.99 | 9.31 |
| | **100** | 99.8 | 1.2 | 6.08 | 0.97 | 10.54 |
| Fast-twitch Fibers | **25** | 23.7 | 5.77 | 1.83 | 1.83 | 1.11 |
| | **50** | 55.5 | 10.1 | 4.70 | 3.66 | 1.57 |
| | **75** | 74.5 | 5.88 | 14.19 | 4.71 | 2.16 |
| | **100** | 98.2 | 1.52 | 27.24 | 4.09 | 4.91 |

*PKA effects on stretch activation in slow-twitch skeletal muscle fibers*

Next we addressed the potential regulatory role that phosphorylation of myofilament proteins by PKA, which in particular has been shown to phosphorylate MyBP-C, plays in stretch activation in slow-twitch skeletal muscle fibers. Our lab has previously observed that PKA-induced phosphorylation of cMyBP-C and cTnI elicited marked increases in transient force overshoots in permeabilized cardiac myocytes preparations (29). To address the molecule specificity of this phenomenon we utilized skinned slow-twitch skeletal muscle fibers, which we have previously shown to be phosphorylated by PKA at MyBP-C sites but not TnI sites (28). We, thus, took this as a model to study the effects of phosphorylating MyBP-C on stretch activation in mammalian skeletal muscle. We hypothesized that PKA treatment would increase $P_{TO}$ over the entire range of $Ca^{2+}$ activation due to phosphorylation of MyBP-C relieving its normal constraint on myosin heads.

The effect of PKA treatment on force redevelopment in slow-twitch skeletal muscle fibers was assessed by measuring the $Ca^{2+}$ dependence of transient overshoot of

force before and after PKA incubation (Fig. 13). (Fiber characteristics are summarized in Table 1)

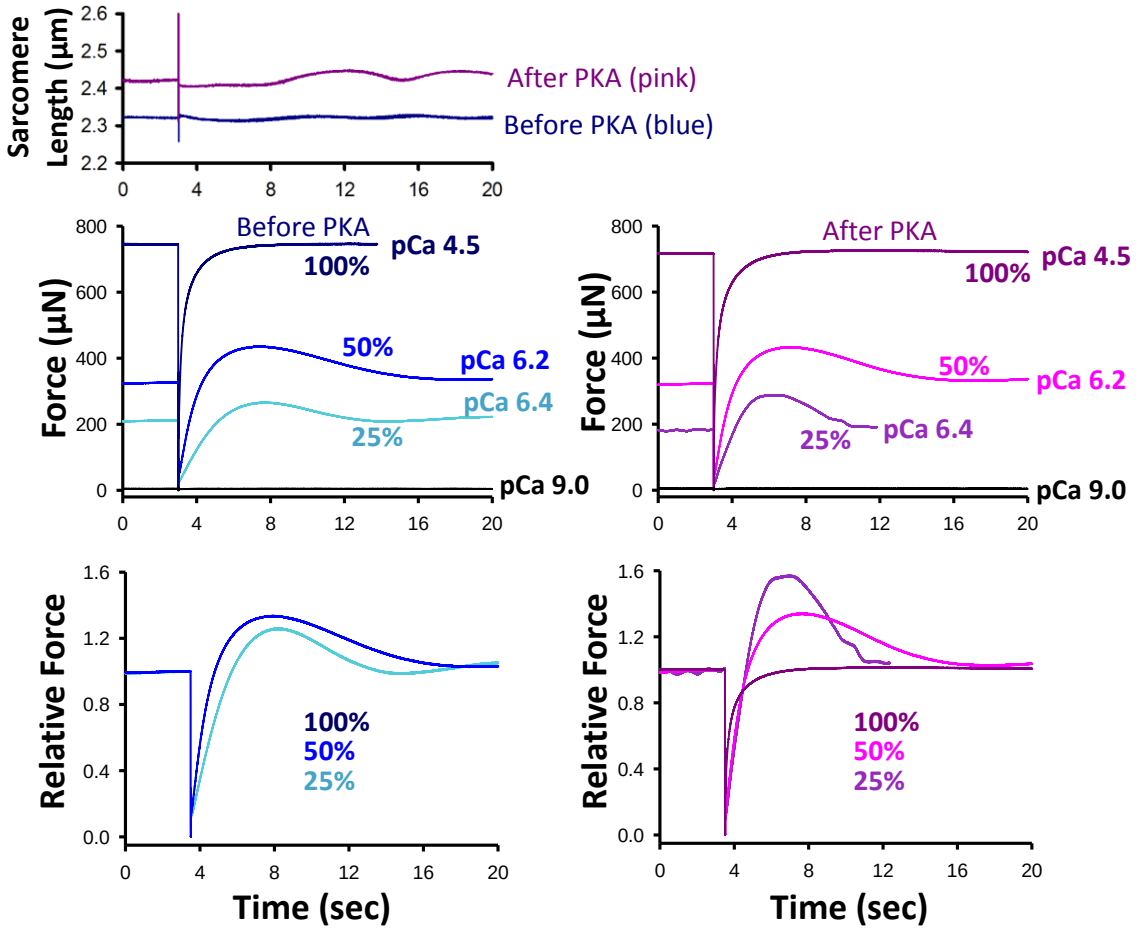


**Figure 13.** *Representative sarcomere length and force redevelopment traces during a slack-re-stretch maneuver in skinned slow-twitch skeletal muscle fibers before and after PKA treatment.* Representative sarcomere length traces before and after PKA treatment. Sarcomere length traces often elicited oscillations following PKA treatment. Representative absolute force traces following a slack-re-stretch maneuver from a slow-twitch skeletal muscle fiber before (blue) and after (pink) treatment with PKA. Representative relative force traces which were normalized to the steady state force before the mechanical perturbation.

Once normalized to steady-state force isometric force, neither the magnitude of the transient force overshoot nor the force redevelopment rates appeared to be changed following PKA treatment at maximal and 50%, 75% and maximal $Ca^{2+}$ activation

levels. However, at low $Ca^{2+}$ activation levels (25% maximal $Ca^{2+}$ activation) both the transient force overshoot and the force redevelopment rate was significantly increased following PKA treatment.

$P_{TO}/P_O$ values were similar before and after PKA treatment at the 50%, 75%, and 100% $Ca^{2+}$ activation levels. However at low $Ca^{2+}$ levels (25%), $P_{TO}$ more than doubled following PKA treatment (Fig. 14). The relative transient force overshoot went from ~19% to ~45% following PKA treatment (all values summarized in Table 3).

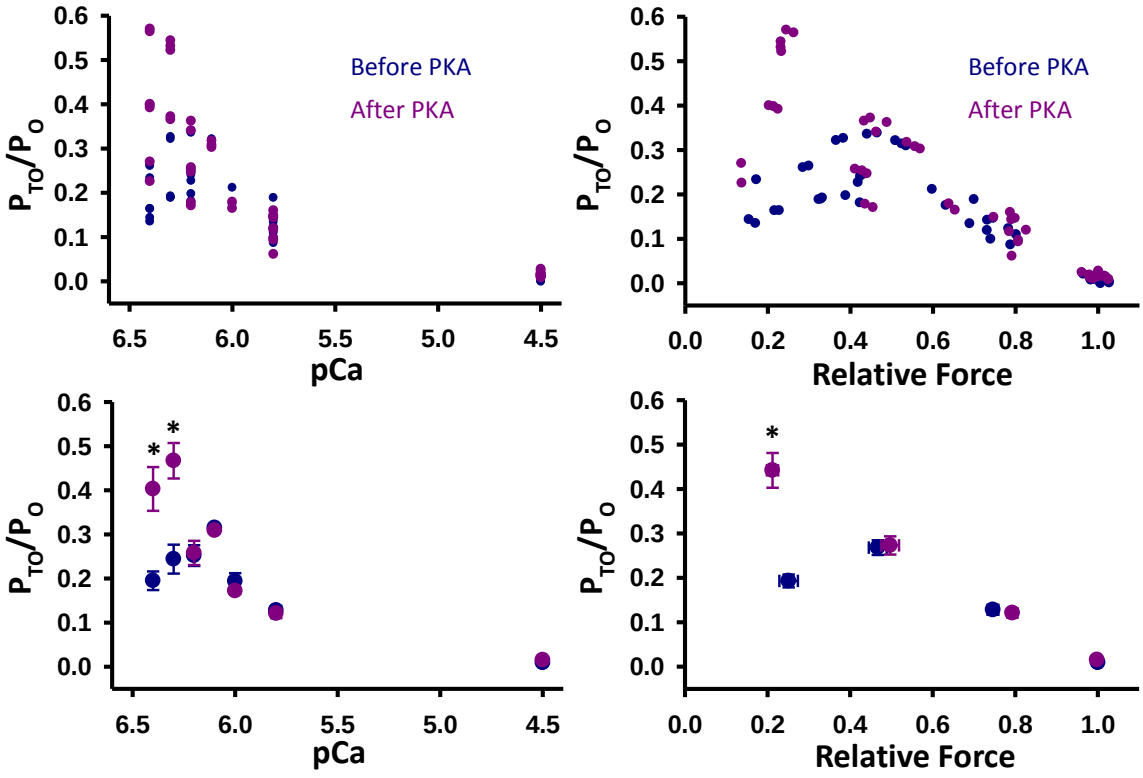


**Figure 14.** *Transient force overshoot ($P_{TO}$) in skinned slow-twitch skeletal muscle fiber preparations before (blue) and after (pink) treatment with PKA as a function of pCa (left) and relative force (right).* Relative transient force overshoot ($P_{TO}/P_O$) is shown as individual points (top) and mean ± bidirectional SEM (bottom). Following PKA treatment, $P_{TO}/P_o$ was significantly greater but only at low levels of $Ca^{2+}$ activation.

Interestingly, force redevelopment rates were also increased after PKA treatment, which has been shown to phosphorylate MyBP-C. However, unlike $P_{TO}$, force redevelopment rates increased over the entire range of $Ca^{2+}$ activation levels (26, 29, 45, 57, 87). The rates of force redevelopment were significantly increased for both the fast phase ($k_1$) (Fig. 15) and the slower phase ($k_2$) (Fig. 16) following PKA treatment. As previously observed, the two phases of force redevelopment converged into one phase at low $Ca^{2+}$ and this occurred both before and after PKA treatment.

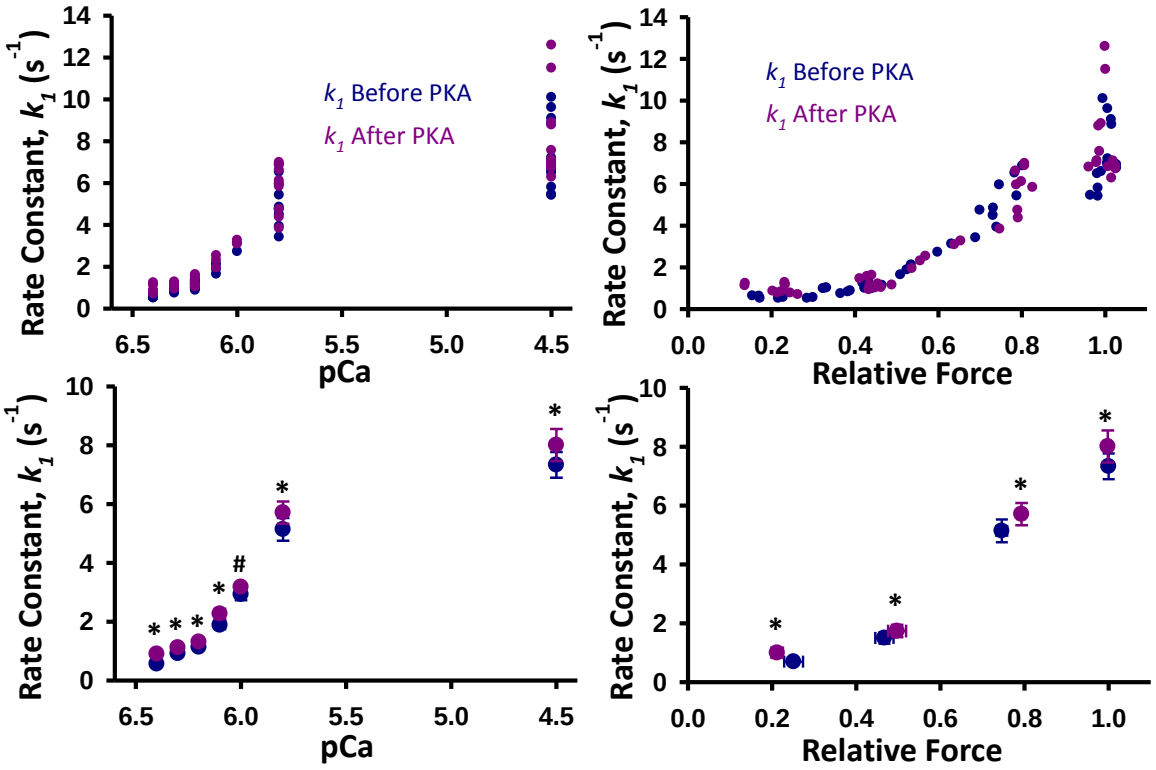


**Figure 15.** *Rates of the fast phase ($k_1$) of force redevelopment before and after PKA.* Rate constants ($s^{-1}$) are shown as both individual data points (top) and mean ± bidirectional SEM (bottom). There was a statistically significant increase in $k_1$ following PKA treatment at all pCa and relative force values. ***** Denotes a statistically significant increase in PKA-induced rate constant vs before PKA treatment. # Denotes significance not resolved due to low power of test.

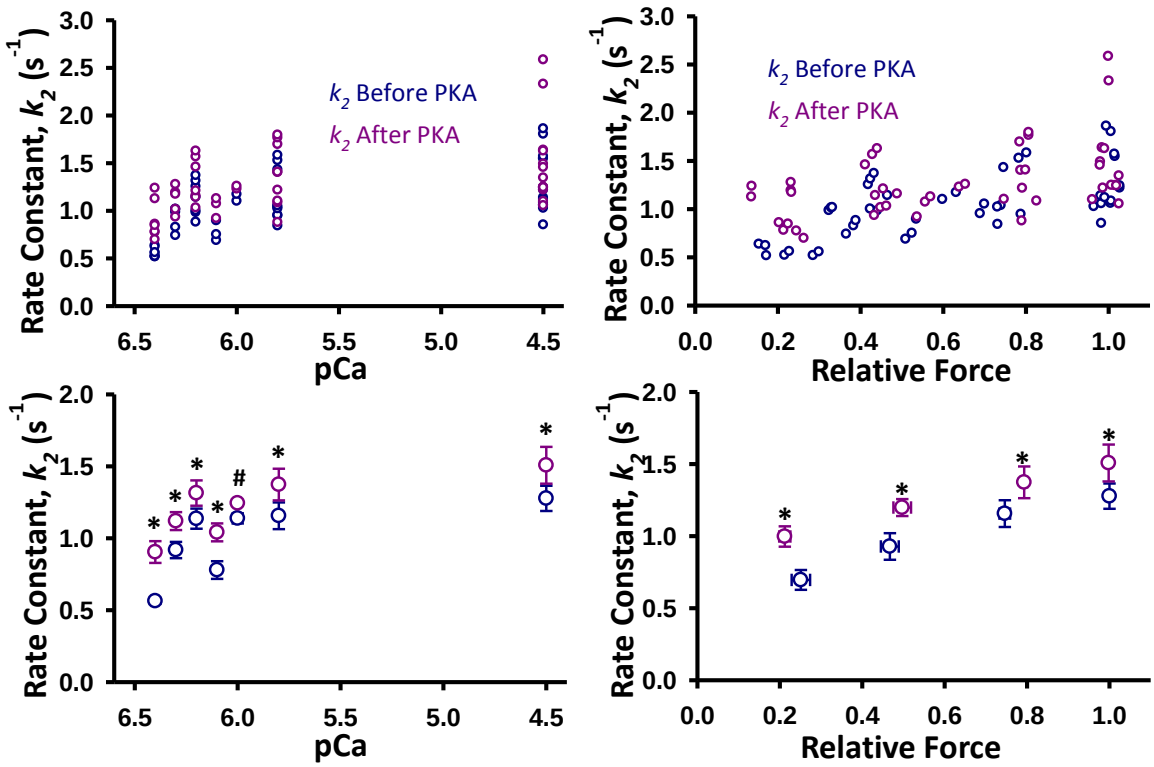


**Figure 16.** *Rates of the slow phase ($k_2$) of force redevelopment before and after PKA.* There was a statistically significant increase in $k_2$ following PKA treatment at all pCa and relative force values. Rate constants ($s^{-1}$) are shown as individual data points (top) and mean ± bidirectional SEM (bottom). *****Denotes a statistically significant increase in PKA-induced rate constant vs before PKA treatment. # Denotes significance not resolved due to low power of test.

In a similar manner as force redevelopment rates, transient force decay rates had a tendency of being faster following PKA treatment. However, $t_{1/2}$ was only significantly smaller following PKA treatment at 50% activation (Fig. 17). Also it should be noted that there was no $t_{1/2}$ value at maximal $Ca^{2+}$ activation. This was due to a lack of transient force overshoot at maximal $Ca^{2+}$.

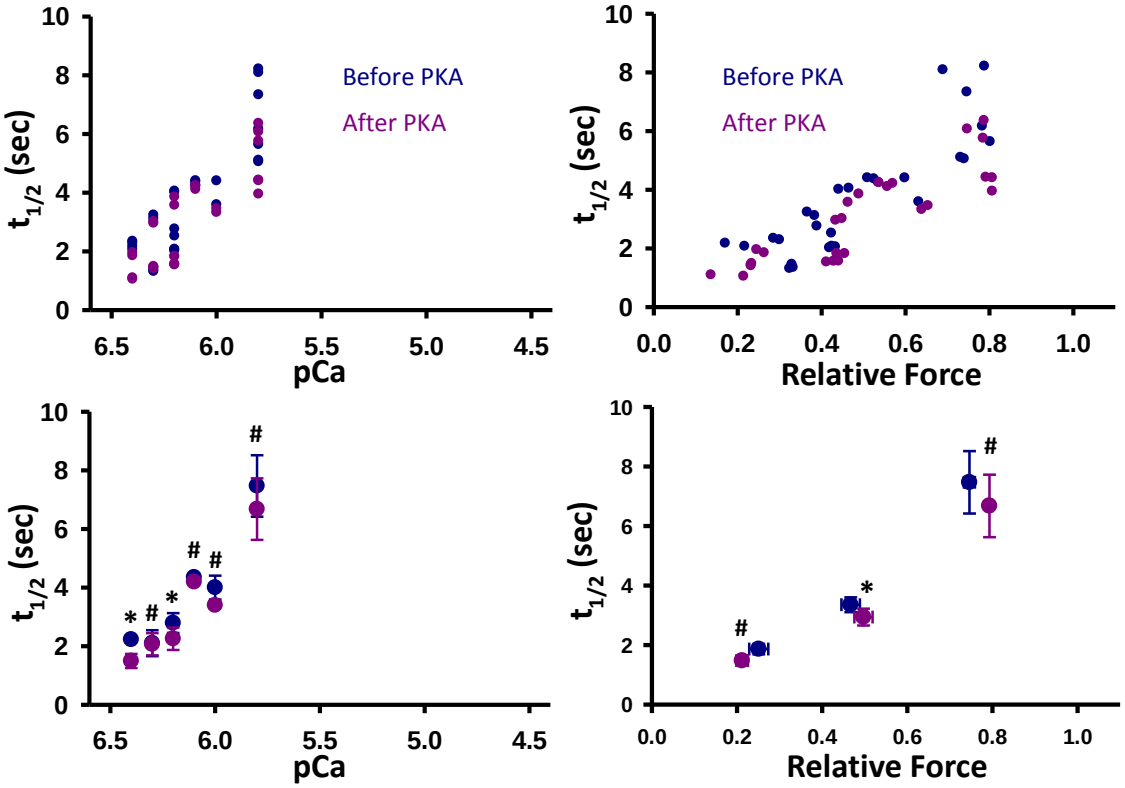


**Figure 17.** *Force decay half-times ($t_{1/2}$) of transient force overshoots. The $t_{1/2}$ values are shown as a function of pCa (left) and relative force (right).* $t_{1/2}$ following PKA treatment had the tendency of being lower (i.e, faster relaxation rates); however, it was only significantly decreased at 50% relative force. The $t_{1/2}$ at ~50% relative force was significantly different from all other values. $t_{1/2}$ values were not recorded at pCa 4.5 (maximum $Ca^{2+}$ activation) due to the lack of a transient force overshoot. # Denotes significance not resolved due to low power of test.

Table 3. Characteristics of Force Redevelopment in Slow-twitch Muscle Fibers Before vs. After PKA Treatment

| | **Rel. Force (%)** | $P_O/P_{4.5}$ (%) | $P_{TO}/P_O$ (%) | $k_1$ ($s^{-1}$) | $k_2$ ($s^{-1}$) | $t_{1/2}$ (sec) |
|---|---|---|---|---|---|---|
| Before PKA | **25** | 25.1 | 19.3 | 0.70 | 0.70 | 1.86 |
| | **50** | 46.7 | 26.8 | 1.50 | 0.93 | 3.35 |
| | **75** | 74.6 | 12.8 | 5.14 | 1.16 | 7.47 |
| | **100** | 100 | 0.923 | 7.33 | 1.28 | - |
| After PKA | **25** | 21.2 | 44.2 | 1.00 | 1.00 | 1.48 |
| | **50** | 49.7 | 27.3 | 1.74 | 1.20 | 2.94 |
| | **75** | 79.3 | 12.1 | 5.71 | 1.37 | 6.68 |
| | **100** | 99.8 | 1.52 | 8.01 | 1.51 | - |

# Discussion

Contraction of striated muscle has long been believed to be regulated through thin filament mechanisms (33). Hitchcock et al. postulated that Tm can exist in two $Ca^{2+}$ dependent states, a "blocked" state in which Tm sterically hinders the acto-myosin interaction or a "closed" state in which $Ca^{2+}$ binding to Tn complex elicits a shift in the Tm position allowing acto-myosin interaction. Tm is now believed to exist in three positions due to myosin binding being required for force generation (49). The blocked and closed states of Tm remain the same in the two models, however, an additional "open" state exists (85). The "open" state of Tm is reached upon binding of force generating cross-bridge. A more recent model encompasses dual filament regulation of contraction has been postulated in recent years (42), by which the thin filament is $Ca^{2+}$ activated, but the thick filament is stress activated. This model was based in part due to the finding that myosin heads in a muscle under a low load remain in an OFF state. This was concluded from x-ray diffractions correlating to the angle of the myosin heads and the periodicity of the thick filament. Under low load state, the thin filament was activated, and the muscle could shorten at max velocity due to the constitutively ON cross-bridges. These findings suggest that $Ca^{2+}$ activation of the thin filament, which has been thought to be the canonical regulator of striated muscle contraction, may not be capable of solely regulating all muscle contraction.

The main focus of this study was to investigate the myofibrillar regulatory mechanisms of stretch activation in mammalian striated muscle. Slow-twitch skeletal muscle fibers elicited greater relative levels of stretch activation ($P_{TO}/P_O$) than the more cooperative fast-twitch skeletal muscle fibers. This result suggests that stretch activation

may not be solely regulated by the extent of apparent cooperative activation of force since stretch activation did not manifest to a greater extent in the more cooperative fiber type. Stretch activation may have not elicited as much of a transient force overshoot in fast-twitch fibers due to their fast force decay rates. The faster rates of force decay would simply not allow enough time to overshoot force. Another possible reason for this variation could be thin filament compliance. According to some computational models, more compliant myofilaments increase recruitment of more force-generating cross-bridges (11) due to additional realignment of myosin binding sites along the filament, which can lead to greater cross-bridge binding and more thin filament cooperative activation by shifting of Tm to open states (14).

Force redevelopment and decay rates were 2-to-4 fold faster in skinned fast-twitch skeletal muscle fibers compared to slow-twitch skeletal muscle fibers, which is consistent with previous studies (4, 51, 69). The finding that force redevelopment was better fit with a double exponential equation suggests that force redevelopment is a biphasic response. If in fact, force redevelopment is a biphasic response, then it may involve a more complex mechanism than can be explained by a simple two-state cross-bridge cycling model as previously postulated (7, 94). Interestingly, the two phases of force redevelopment converge at low levels of $Ca^{2+}$ activation. The rate constant of the faster process ($k_1$) was more $Ca^{2+}$ activation dependent than rate constant of the slower process ($k_2$). Cooperative activation is thought to be a slow process indicative of $k_2$. $k_1$ is likely a result of the cycling kinetics of the cross-bridges from detached to attached and force generating states and vice versa. At higher levels of steady-state $Ca^{2+}$ activation, there is a higher probability that considerable regions of both the thin and thick filaments

are activated such that the first order process of cross-bridge cycling limits the rate of force development. However, at lower levels of $Ca^{2+}$ activation more regions of both the thin and thick filament are in the off state and necessitate cooperative activation, which takes considerably more time in relation to cross-bridge cycling per se. Force decay rates were faster and less $Ca^{2+}$ activation dependent in fast-twitch skeletal muscle. The lower $Ca^{2+}$ dependence of transient force decay rates in fast-twitch skeletal muscle fibers may arise because fast-twitch skeletal muscle fibers have evolved a myofibrillar system that inactivates both its thin and thick filaments in a highly coordinated, cooperative switch-like fashion to assist in its rapid relaxation and explosive contraction required for physiological function of that muscle type.

Following PKA treatment, skinned slow-twitch skeletal muscle fibers elicited a doubling of $P_{TO}/P_O$ (19% to 44%) at low $Ca^{2+}$ activation (25%). This is consistent with the theory of dual filament regulation of contraction (42) (Fig. 3). When the muscle is exposed to low stress (low $Ca^{2+}$) the thin filament is activated, but the majority of the thick filament remains in the OFF state. Thus at low levels of stress or force, there remains a large pool of cross-bridges available for force generation. With regards to the role of MyBP-C and its phosphorylation by PKA in a relaxed/low stress state, the M domain of MyBP-C has a high affinity for the S2 region of the myosin which suppresses the myosin head increases its propensity to the OFF state (Fig. 18 left). Based on biochemical studies quantifying cMyBP-C binding constants to myosin and actin, PKA-induced phosphorylation of MyBP-C has been modeled to cause a shift in its M domain affinity from the myosin head to actin, which may increase the probability of myosin cross-bridges making the transition for the OFF to the ON state. The myosin heads are

now primed for and more readily available for force generation (Fig. 18 right) by lowering the threshold of stress/strain required to activate the thick filament. This large pool of available cross-bridges may contribute to greater stretch activation. PKA-induced phosphorylation of MyBP-C also elicited accelerated force redevelopment rates. This may be due to an increase in the cross-bridge cycling kinetics or faster rates of either think or thick filament activation (82, 87). With increased faster force redevelopment rates likely due, at least in part, to increase in cross-bridge cycling kinetics (87), it might be expected that the force decay rates would be faster as well. However, this was not observed at all $Ca^{2+}$ activation levels, which may imply that MyBP-C phosphorylation may favor activation processes over inactivation processes.

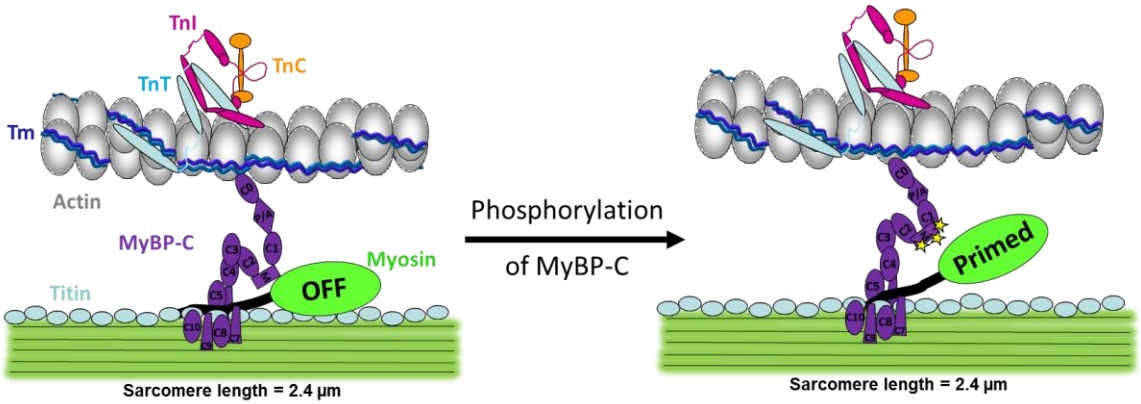


**Figure 18.** *MyBP-C regulation of Stretch Activation.* In a relaxed state, MyBP-C suppresses the myosin head in the OFF state (left). Upon phosphorylation MyBP-C's binding affinity is turned in favor of actin, which primes the myosin head to be available for force generation (right).

Insect flight muscle and mammalian striated muscle differ structurally; however, they may regulate stretch activation via similar mechanisms. Albeit IFM is theorized to regulate stretch activation via a thin filament mechanism, it is proposed in this thesis that stretch activation in mammalian striated muscle, at least in part, is regulated via a thick

filament mechanism. It appears that there potentially is a molecular suppressor of contractile proteins in both muscle types, i.e. Tn-bridges in IFM and MyBP-C in mammalian striated muscle. A proposed regulator of stretch activation in insect flight muscle is the Tn-bridges (10, 58). In this model (Fig. 4), the Tn-bridges sterically hinder the thin filament to prevent full activation of the thin filament at low stress. Under low stress, there are only weakly bound cross-bridges present. Upon stretch, the troponin bridges are pulled which allows Tm to shift into the open state and the formation of strongly bound cross-bridges. In a similar manner, MyBP-C may be a regulator of stretch activation in skeletal muscle. As previously stated, MyBP-C has a high binding affinity for the S2 region of myosin and is also bound to actin. In this model (Fig. 18), the high binding affinity of MyBP-C for myosin could sterically hinder myosin heads from interacting with actin and undergoing force-generating transitions. However, upon MyBP-C phosphorylation, its inhibitory affect is alleviated, which may elicit greater degrees of stretch activation. While these molecules and their primary filament of interaction differ between IFM and mammalian striated muscle, in essence, they may have similar roles in regulating stretch activation. Although the phosphorylation of MyBP-C appears to play a role in the regulation of stretch activation, it remains possible that PKA phosphorylation of other myofibrillar proteins may contribute to the observed increase in the transient tension overshoot. For example, titin is a known substrate for PKA and its PKA-mediated phosphorylation has been shown to cause increase titin extensibility and reduce passive force (25). However, it seems counter intuitive that a more compliant titin molecule would in fact augment stretch activation. In fact, previous (unpublished data) from our laboratory found that trypsin mediated cleavage of titin

molecules actually eliminated transient tension overshoots (Schuster, J.M., The University of Missouri Master's Thesis, "The contribution of titin to striated muscle shortening"). One way to more directly test the role of other myofibrillar PKA substrates on stretch activation would be to administer PKA to skinned skeletal muscle fiber preparations lacking MyBP-C.

Stretch activation function is known to contribute to the regulation of oscillatory muscle contraction, i.e. sinusoidal muscle contractions of IFM and mammalian cardiac muscle. Skeletal muscle is generally thought to not be an oscillatory muscle, which may be why relative stretch-activated force is not as great in skeletal muscle. However, spontaneous oscillatory contractions (SPOCs) have been reported in a number of studies examining the mechanics of permeabilized cardiac myocyte preparations and skeletal muscle fibers (72, 84). Interestingly, in this study we observed that PKA treatment both markedly increased the number of SPOCs and yielded greatest relative transient force overshoots in skinned slow-twitch skeletal muscle fibers. A similar phenomenon has been reported in rat skinned cardiac myocyte preparations (29). The relationship between SPOCs and stretch activation and whether they share similar molecular mechanism requires additional studies.

Future studies to further assess stretch activation and its potential underlying mechanism include perhaps starting with a comparative study of permeabilized IFM, cardiac muscle, and slow-twitch and fast-twitch skeletal muscle using the same methodology in order to quantify the amplitude and kinetics of stretch activation between muscle types. Additional experiments could incorporate a high molecular weight polymer such as dextran to compress the myofilament lattice towards values more closely

associated with intact muscle (42, 72). Dextran is thought to cause the thick filament to favor the OFF state (19), thus the presence of dextran is hypothesized to elicit smaller transient force overshoots in skinned slow-twitch skeletal muscle fibers; however, following PKA treatment there will be a pronounced increase in relative transient force overshoot. It has been proposed that titin not only contributes to passive tension, but also active force generation through the extension and refolding titin domains (66). The extension and refolding of the domains could contribute to stretch activation. Blebbistatin, a known suppressor of the thick filament (19), would provide a model for testing titin's contribution to stretch activation in a $Ca^{2+}$ activated muscle. Additional experiments could quantify the role of thick and thin filament proteins in the marked increase in transient force overshoots observed in skinned cardiac myocyte preparations (29). For instance, since slow-twitch skeletal TnI does not contain PKA site, cardiac TnI with pseudophosphorylated PKA sites could be exchanged into skinned slow-twitch skeletal muscle fibers. The effects of this exchange on transient force overshoots before and after PKA treatment would provide a quantitative assessment of the role of each protein and whether the effects elicit a zero sum, additive, or synergistic gain. Using a cMyBP-C ablation mouse model, stretch activation was found to be enhanced in skinned myocardial preparations (79). It is hypothesized that the addition of MyBP-C molecules to the skinned muscle preparations lacking MyBP-C would attenuate stretch activation capability.

Overall, work from this thesis found evidence for stretch activation in both permeabilized fast-twitch and slow-twitch skeletal muscle fibers. Stretch activation, which was quantified as transient force overshoot after slack-re-stretch maneuver, has

been hypothesized to arise from cooperative activation of the thin filament (12). If in fact, stretch activation is a result of cooperative activation of the thin filament, then we hypothesized that skinned fast-twitch fibers would elicit greater stretch activation due to its higher relative level of cooperativity. Contrary to our hypothesis, transient force overshoots were greater in the less cooperative slow-twitch skeletal muscle fiber, which suggests that stretch activation may not be solely due to the extent of apparent cooperative activation of force in myofilament system. Following slack-re-stretch maneuver, force redevelopment rates were quantified and found to be best fit with a double exponential equation. Interestingly, at low $Ca^{2+}$ activation levels (25%), the two phases of force redevelopment converged into one process. The rate of relaxation of the transient force overshoot also was quantified (by time to half of force decay ($t_{1/2}$)) and was considerable faster but less $Ca^{2+}$ activation dependent in fast-twitch skeletal muscle fiber preparations. Next, the role of PKA-mediated MyBP-C phosphorylation on stretch activation was assessed using slow-twitch skeletal muscle fibers. Interestingly, the transient force overshoot increased by greater than two-fold following PKA treatment at low levels of $Ca^{2+}$ activation. In addition, force redevelopment rates were significantly increased across the entire range of $Ca^{2+}$ activation levels. In a similar manner, transient force decay rates had a tendency of being faster following PKA treatment. Overall, these are consistent with a model whereby stretch transiently increases the number of cross-bridges made available for force generation and PKA phosphorylation of MyBP-C enhances these stretch activation processes. These results are consistent with a regulation of contraction model whereby MyBP-C has an inhibitory role on the myosin cross-bridges, which may be relieved following phosphorylation. Future studies are needed to

provide a more complete mechanistic understanding of stretch activation in mammalian striated muscle during normal contractions and how these regulatory processes are altered with acute increases in metabolic demands and by chronic changes in muscle function associated with exercise training and disease states.

# References


1. **Ababou A, Rostkova E, Mistry S, Le Masurier C, Gautel M, and Pfuhl M.** Myosin binding protein C positioned to play a key role in regulation of muscle contraction: structure and interactions of domain C1. *Journal of Molecular Biology* 384: 615-630, 2008.

2. **Ackermann MA and Kontrogianni-Konstantopoulos A.** Myosin binding protein-C slow is a novel substrate for protein kinase A (PKA) and C (PKC) in skeletal muscle. *Journal of Proteome Research* 10: 4547-4555, 2011.

3. **Bailey K.** Tropomyosin: a new asymmetric protein component of the muscle fibril. *Biochem J* 43: 271-279, 1948.

4. **Barany M.** ATPase activity of myosin correlated with speed of muscle shortening. *Journal of General Physiology* 50: 197-216, 1967.

5. **Barefield D and Sadayappan S.** Phosphorylation and function of cardiac myosin binding protein-C in health and disease. *Journal of Molecular & Cellular Cardiology* 48: 866-875, 2010.

6. **Bennett P, Craig R, Starr R, and Offer G.** The ultrastructural location of C-protein, X-protein, and H-protein in rabbit muscle. *Journal of Muscle Research and Cell Motility* 7: 550-567, 1986.

7. **Brenner B.** Effect of calcium on cross-bridge turnover kinetics in skinned single rabbit psoas fibers: implications for regulation of muscle contraction. *Proceedings of the National Academy of Sciences* 85: 3265-3269, 1988.

8. **Brenner B.** Mechanical and structural approaches to correlation of cross-bridge action in muscle with actomyosin ATPase in solution. *Annu Rev Physiol* 49: 655-672, 1987.

9. **Bullard B, Leonard K, Larkins A, Butcher G, Karlik C, and Fyrberg E.** Troponin of asynchronous flight muscle. *J Mol Biol* 204: 621-637, 1988.

10. **Bullard B and Pastore A.** Regulating the contraction of insect flight muscle. *J Muscle Res Cell Motil* 32: 303-313, 2011.

11. **Campbell KS.** Filament compliance effects can explain tension overshoots during force development. *Biophysical Journal* 91: 4102-4109, 2006.

12. **Campbell KS.** Tension recovery in permeabilized rat soleus muscle fibers after rapid shortening and restretch. *Biophysical Journal* 90: 1288-1294, 2006.

13. **Cooke R.** Actomyosin interaction in striated muscle. *Physiological Reviews* 77: 671-697, 1997.

14. **Daniel TL, Trimble AC, and Chase PB.** Compliant realignment of binding sites in muscle: transient behavior and mechanical tuning. *Biophys J* 74: 1611-1621, 1998.

15. **Davis JS, Hassanzadeh S, Winitsky S, Lin H, Satorius C, Vemuri R, Aletras AH, Wen H, and Epstein ND.** The overall pattern of cardiac contraction depends on a spatial gradient of myosin regulatory light chain phosphorylation. *Cell* 107: 631-641, 2001.

16. **Epstein ND and Davis JS.** When is a fly in the ointment a solution and not a problem? *Circ Res* 98: 1110-1112, 2006.

17. **Ford LE, Huxley AF, and Simmons RM.** The relation between stiffness and filament overlap in stimulated frog muscle fibres. *J Physiol* 311: 219-249, 1981.

18. **Fukuda N, Wu Y, Nair P, and Granzier HL.** Phosphorylation of titin modulates passive stiffness of cardiac muscle in a titin isoform-dependent manner. *Journal of General Physiology* 125: 249-252, 2005.

19. **Fusi L, Brunello E, Yan Z, and Irving M.** Thick filament mechano-sensing is a calcium-independent regulatory mechanism in skeletal muscle. *Nat Commun* 7: 13281, 2016.

20. **Galler S, Schmitt TL, and Pette D.** Stretch activation, unloaded shortening velocity, and myosin heavy chain isoforms of rat skeletal muscle fibres. *J Physiol* 478 Pt 3: 513-521, 1994.

21. **Gardetto PR, Schluter JM, and Fitts RH.** Contractile function of single muscle fibers after hindlimb suspension. *J Appl Physiol (1985)* 66: 2739-2749, 1989.

22. **Gomes AV, Venkatraman G, Davis JP, Tikunova SB, Engel P, Solaro RJ, and Potter JD.** Cardiac troponin T isoforms affect the Ca(2+) sensitivity of force development in the presence of slow skeletal troponin I: insights into the role of troponin T isoforms in the fetal heart. *J Biol Chem* 279: 49579-49587, 2004.

23. **Gordon AM, Homsher E, and Regnier M.** Regulation of contraction in striated muscle. *Physiological Reviews* 80: 853-924, 2000.

24. **Granzier HL and Irving TC.** Passive tension in cardiac muscle: Contribution of collagen, titin, microtubules, and intermediate filaments. *Biophysical Journal* 68: 1027-1044, 1995.

25. **Granzier HL and Labeit S.** The giant protein titin: a major player in myocardial mechanics, signaling, and disease. *Circulation Research* 94: 284-295, 2004.

26. **Gresham KS, Mamidi R, and Stelzer JE.** The contribution of cardiac myosin binding protein-C ser282 phosphorylation to the rate of force generation and in vivo cardiac contractility. *Journal of Physiology* 592: 3747-3765, 2014.

27. **Hanft LM, Biesiadecki BJ, and McDonald KS.** Length dependence of striated muscle force generation is controlled by phosphorylation of cTnI at serines 23/24. *Journal of Physiology* 591: 4535-4547, 2013.

28. **Hanft LM, Cornell TD, McDonald CA, Rovetto MJ, Emter CA, and McDonald KS.** Molecule specific effects of PKA-mediated phosphorylation on rat isolated heart and cardiac myofibrillar function. *Archives of Biochemistry and Biophysics* 601: 22-31, 2016.

29. **Hanft LM and McDonald KS.** Sarcomere length dependence of power output is increased after PKA treatment in rat cardiac myocytes. *American Journal of Physiology Heart & Circulatory Physiology* 296: H1524-H1531, 2009.

30. **Hartshorne DJ and Mueller H.** Fractionation of troponin into two distinct proteins. *Biochem Biophys Res Commun* 31: 647-653, 1968.

31. **Hartzell HC and Sale WS.** Structure of C protein purified from cardiac muscle. *Journal of Cell Biology* 100: 208-215, 1985.

32. **Herzberg O and James MN.** Structure of the calcium regulatory muscle protein troponin-C at 2.8 A resolution. *Nature* 313: 653-659, 1985.

33. **Hitchcock SE, Huxley HE, and Szent-Gyorgyi AG.** Calcium sensitive binding of troponin to actin-tropomyosin: a two-site model for troponin action. *J Mol Biol* 80: 825-836, 1973.

34. **Hofmann PA, Greaser ML, and Moss RL.** C-protein limits shortening velocity of rabbit skeletal muscle fibres at low levels of calcium activation. *Journal of Physiology* 439: 701-715, 1991.

35. **Huxley HE.** Electron microscope studies of the organisation of the filaments in striated muscle. *Biochim Biophys Acta* 12: 387-394, 1953.

36. **Josephson RK, Malamud JG, and Stokes DR.** Asynchronous muscle: a primer. *J Exp Biol* 203: 2713-2722, 2000.

37. **Kendrick-Jones J, Smith RC, Craig R, Cande WZ, Tooth PJ, and Scholey JM.** The role of myosin light chain phosphorylation in the regulation of contractile activity. *Biochem Soc Trans* 11: 154, 1983.

38. **Korte FS, McDonald KS, Harris SP, and Moss RL.** Loaded shortening, power output, and rate of force redevelopment are increased with knockout of cardiac myosin binding protein-C. *Circulation Research* 93: 752-758, 2003.

39. **Kress M, Huxley HE, Faruqi AR, and Hendrix J.** Structural changes during activation of frog muscle studied by time-resolved X-ray diffraction. *Journal of Molecular Biology* 188: 325-342, 1986.

40. **Kumar M, Govindan S, Zhang M, Khairallah RJ, Martin JL, Sadayappan S, and De Tombe PP.** Cardiac myosin-binding protein C and troponin-I phosphorylation independently modulate myofilament length-dependent activation. *Journal of Biological Chemistry* 290: 29241-29249, 2015.

41. **Lehman W, Medlock G, Li XE, Suphamungmee W, Tu AY, Schmidtmann A, Ujfalusi Z, Fischer S, Moore JR, Geeves MA, and Regnier M.** Phosphorylation of

Ser283 enhances the stiffness of the tropomyosin head-to-tail overlap domain. *Arch Biochem Biophys* 571: 10-15, 2015.

42. **Linari M, Brunello E, Reconditi M, Fusi L, Caremani M, Narayanan T, Piazzesi G, Lombardi V, and Irving M.** Force generation by skeletal muscle is controlled by mechanosensing in myosin filaments. *Nature* 528: 276-279, 2015.

43. **Linari M, Reedy MK, Reedy MC, Lombardi V, and Piazzesi G.** Ca-activation and stretch-activation in insect flight muscle. *Biophys J* 87: 1101-1111, 2004.

44. **Malhotra A, Nakouzi A, J. B, and Buttrick PM.** Expression and regulation of mutant forms of cardiac TnI in a reconstituted actomyosin system: role of kinase dependent phosphorylation. *Molecular & Cellular Biochemistry* 170: 99-107, 1997.

45. **Mamidi R, Gresham KS, Verma S, and Stelzer JE.** Cardiac myosin binding protein-C phosphorylation modulates myofilament length-dependent activation. *Frontiers Physiology* 7: Article 38, 2016.

46. **Marden JH.** Variability in the size, composition, and function of insect flight muscles. *Annu Rev Physiol* 62: 157-178, 2000.

47. **McDonald KS.** $Ca^{2+}$ dependence of loaded shortening in rat skinned cardiac myocytes and skeletal muscle fibers. *Journal of Physiology* 525: 169-181, 2000.

48. **McDonald KS and Fitts RH.** Effect of hindlimb unweighting on single soleus fiber maximal shortening velocity and ATPase activity. *Journal of Applied Physiology* 74: 2949-2957, 1993.

49. **McKillop DF and Geeves MA.** Regulation of the interaction between actin and myosin subfragment 1: evidence for three states of the thin filament. *Biophysical Journal* 65: 693-701, 1993.

50. **Metzger JM, Greaser ML, and Moss RL.** Variations in cross-bridge attachment rate and tension with phosphorylation of myosin in mammalian skinned skeletal muscle fibers: implications for twitch potentiation in intact muscle. *Journal of General Physiology* 93: 855-883, 1989.

51. **Metzger JM and Moss RL.** Calcium-sensitive cross-bridge transitions in mammalian fast and slow skeletal muscle fibers. *Science* 247: 1088-1090, 1990.

52. **Miller CJ, Cheung P, White P, and Reisler E.** Actin's view of actomyosin interface. *Biophys J* 68: 50S-54S, 1995.

53. **Moos C, Mason CM, Besterman JM, Feng IN, and Dubin JH.** The binding of skeletal muscle C-protein to F-actin, and its relation to the interaction of actin with myosin subfragment-1. *Journal of Molecular Biology* 124: 571-586, 1978.

54. **Moos C, Offer G, Starr R, and Bennett P.** Interaction of C-protein with myosin, myosin rod and light meromyosin. *Journal of Molecular Biology* 97: 1-9, 1975.

55. **Moss RL, Razumova MV, and Fitzsimons DP.** Myosin crossbridge activation of cardiac thin filaments: Implications for myocardial function in health and disease. *Circulation Research* 94: 1290-1300, 2004.

56. **Pan BS, Gordon AM, and Luo ZX.** Removal of tropomyosin overlap modifies cooperative binding of myosin S-1 to reconstituted thin filaments of rabbit striated muscle. *J Biol Chem* 264: 8495-8498, 1989.

57. **Patel JR, Fitzsimons DP, Buck SH, Muthuchamy M, Wieczorek DF, and Moss RL.** PKA accelerates rate of force development in murine skinned myocardium expressing alpha- or beta-tropomyosin. *American Journal of Physiology Heart & Circulatory Physiology* 280: H2732-H2739, 2001.

58. **Perz-Edwards RJ, Irving TC, Baumann BA, Gore D, Hutchinson DC, Krzic U, Porter RL, Ward AB, and Reedy MK.** X-ray diffraction evidence for myosin-troponin connections and tropomyosin movement during stretch activation of insect flight muscle. *Proc Natl Acad Sci U S A* 108: 120-125, 2011.

59. **Piazzesi G, Reconditi M, Linari M, Lucii L, Bianco P, Brunello E, Decostre V, Stewart A, Gore DB, Irving TC, Irving M, and Lombardi V.** Skeletal muscle performance determined by modulation of number of myosin motors rather than motor force or stroke size. *Cell* 131: 784-795, 2007.

60. **Poole KJ, Lorenz M, Evans G, Rosenbaum G, Pirani A, Craig R, Tobacman LS, Lehman W, and Holmes KC.** A comparison of muscle thin filament models obtained from electron microscopy reconstructions and low-angle X-ray fibre diagrams from non-overlap muscle. *J Struct Biol* 155: 273-284, 2006.

61. **Pringle JW.** The Croonian Lecture, 1977. Stretch activation of muscle: function and mechanism. *Proc R Soc Lond B Biol Sci* 201: 107-130, 1978.

62. **Pringle JW.** The excitation and contraction of the flight muscles of insects. *J Physiol* 108: 226-232, 1949.

63. **Pyle WG and Solaro RJ.** At the crossroads of myocardial signaling: the role of Z-discs in intracellular signaling and cardiac function. *Circ Res* 94: 296-305, 2004.

64. **Qiu F, Lakey A, Agianian B, Hutchings A, Butcher GW, Labeit S, Leonard K, and Bullard B.** Troponin C in different insect muscle types: identification of two isoforms in Lethocerus, Drosophila and Anopheles that are specific to asynchronous flight muscle in the adult insect. *Biochem J* 371: 811-821, 2003.

65. **Rayment I, Rypniewski WR, Schmidt-Base K, Smith R, Tomchick DR, Benning MM, Winkelmann DA, Wesenberg G, and Holden HM.** Three-dimensional structure of myosin subfragment-1: a molecular motor. *Science* 261: 50-58, 1993.

66. **Rivas-Pardo JA, Eckels EC, Popa I, Kosuri P, Linke WA, and Fernandez JM.** Work Done by Titin Protein Folding Assists Muscle Contraction. *Cell Rep* 14: 1339-1347, 2016.

67. **Robertson SP, Johnson JD, Holroyde MJ, Kranias EG, Potter JD, and Solaro RJ.** The effect of troponin I phosphorylation on the $Ca^{2+}$ -binding properties of the $Ca^{2+}$-regulatory site of bovine cardiac troponin. *Journal of Biological Chemistry* 257: 260-263, 1982.

68. **Ruegg JC, Steiger GJ, and Schadler M.** Mechanical activation of the contractile system in skeletal muscle. *Pflugers Arch* 319: 139-145, 1970.

69. **Schiaffino S and Reggiani C.** Molecular diversity of myofibrillar proteins: gene regulation and functional significance. *Physiol Rev* 76: 371-423, 1996.

70. **Schutt CE, Myslik JC, Rozycki MD, Goonesekere NC, and Lindberg U.** The structure of crystalline profilin-beta-actin. *Nature* 365: 810-816, 1993.

71. **Sheikh F, Ouyang K, Campbell SG, Lyon RC, Chuang J, Fitzsimons DP, Tangney JR, Hidalgo CG, Chung CS, Cheng H, Dalton ND, Gu Y, Kasahara H, Ghassemain M, Omens JH, Peterson KL, Granzier HL, Moss RL, McCulloch AD, and Chen J.** Mouse and computational models link Mlc2v dephosphorylation to altered myosin kinetics in early cardiac disease. *Journal of Clinical Investigation* 122: 1209-1221, 2012.

72. **Shimamoto Y, Suzuki M, and Ishiwata S.** Length-dependent activation and auto-oscillation in skeletal myofibrils at partial activation by Ca2+. *Biochem Biophys Res Commun* 366: 233-238, 2008.

73. **Simmons RM and Szent-Gyorgyi AG.** A mechanical study of regulation in the striated adductor muscle of the scallop. *J Physiol* 358: 47-64, 1985.

74. **Smith DA and Stephenson DG.** The mechanism of spontaneous oscillatory contractions in skeletal muscle. *Biophys J* 96: 3682-3691, 2009.

75. **Solaro RJ and Rarick HM.** Troponin and tropomyosin: proteins that switch on the tune in the activity of cardiac myofilaments. *Circulation Research* 83: 471-480, 1998.

76. **Starr R and Offer G.** The interaction of C-protein with heavy meromyosin and subfragment-2. *Biochemical Journal* 171: 813-816, 1978.

77. **Starr R and Offer G.** Polypeptide chains of intermediate molecular weight in myosin preparations. *FEBS Letters* 15: 40-44, 1971.

78. **Steiger GJ.** Stretch activation and myogenic oscillation of isolated contractile structures of heart muscle. *Pflugers Arch* 330: 347-361, 1971.

79. **Stelzer JE, Dunning SB, and Moss RL.** Ablation of Cardiac Myosin-Binding Protein-C Accelerates Stretch Activation in Murine Skinned Myocardium. Circ Res, 2006, p. 1212-1218.

80. **Stelzer JE, Larsson L, Fitzsimons DP, and Moss RL.** Activation Dependence of Stretch Activation in Mouse Skinned Myocardium: Implications for Ventricular Function. J Gen Physiol, 2006, p. 95-107.

81. **Stelzer JE and Moss RL.** Contributions of stretch activation to length-dependent contraction in murine myocardium. *J Gen Physiol* 128: 461-471, 2006.

82. **Stelzer JE, Patel JR, and Moss RL.** Acceleration of Stretch Activation in Murine Myocardium due to Phosphorylation of Myosin Regulatory Light Chain. J Gen Physiol, 2006, p. 261-272.

83. **Stelzer JE, Patel JR, and Moss RL.** Protein Kinase A-Mediated Acceleration of the Stretch Activation Response in Murine Skinned Myocardium Is Eliminated by Ablation of cMyBP-C. *Circulation Research* 99: 884-890, 2006.

84. **Stephenson DG and Williams DA.** Effects of sarcomere length on the force-pCa relation in fast- and slow-twitch skinned muscle fibers from the rat. *Journal of Physiology* 333: 637-653, 1982.

85. **Tardiff JC.** Thin filament mutations: developing an integrative approach to a complex disorder. *Circulation Research* 108: 765-782, 2011.

86. **Tobacman L.** Thin filament-mediated regulation of cardiac contraction. *Annual review of Physiology* 58: 447-481, 1996.

87. **Tong CW, Stelzer JE, Greaser ML, Powers PA, and Moss RL.** Acceleration of crossbridge kinetics by protein kinase A phosphorylation of cardiac myosin binding protein C modulates cardiac function. *Circulation Research* 103: 974-982, 2008.

88. **Tregear RT, Edwards RJ, Irving TC, Poole KJ, Reedy MC, Schmitz H, Towns-Andrews E, and Reedy MK.** X-ray diffraction indicates that active cross-bridges bind to actin target zones in insect flight muscle. *Biophys J* 74: 1439-1451, 1998.

89. **Trinick J.** Titin as a scaffold and spring. Cytoskeleton. *Curr Biol* 6: 258-260, 1996.

90. **van der Velden J, Papp Z, Boontje NM, Zaremba R, de Jong JW, Janssen PM, Hasenfuss G, and Stienen GJ.** The effect of myosin light chain 2

dephosphorylation on $Ca^{2+}$-sensitivity of force is enhanced in failing human hearts. *Cardiovascular Research* 57: 505-514, 2003.

91. **Vemuri R, Lankford EB, Poetter K, Hassanzadeh S, Takeda K, Yu ZX, Ferrans VJ, and Epstein ND.** The stretch-activation response may be critical to the proper functioning of the mammalian heart. *Proc Natl Acad Sci U S A* 96: 1048-1053, 1999.

92. **Wang K, McClure J, and Tu A.** Titin: major myofibrillar components of striated muscle. *Proceedings of the National Academy of Sciences USA* 76: 3698-3702, 1979.

93. **Wang Q, Zhao C, and Swank DM.** Calcium and stretch activation modulate power generation in Drosophila flight muscle. *Biophys J* 101: 2207-2213, 2011.

94. **Wolff MR, McDonald KS, and Moss RL.** Rate of tension development in cardiac muscle varies with level of activator calcium. *Circulation Research* 76: 154-160, 1995.